Atmospheric
Chemistry
and Physics

MIX: a mosaic Asian anthropogenic emission inventory under the international collaboration framework of the MICS-Asia and HTAP

Meng Li[1,2], **Qiang Zhang**[1,12], **Jun-ichi Kurokawa**[3], **Jung-Hun Woo**[4], **Kebin He**[2,11,12], **Zifeng Lu**[5], **Toshimasa Ohara**[6], **Yu Song**[7], **David G. Streets**[5], **Gregory R. Carmichael**[8], **Yafang Cheng**[9], **Chaopeng Hong**[1,2], **Hong Huo**[10], **Xujia Jiang**[1,2], **Sicong Kang**[2], **Fei Liu**[2], **Hang Su**[9], and **Bo Zheng**[2]

[1]Ministry of Education Key Laboratory for Earth System Modeling, Department of Earth System Science, Tsinghua University, Beijing, China
[2]State Key Joint Laboratory of Environment Simulation and Pollution Control, School of Environment, Tsinghua University, Beijing, China
[3]Asia Center for Air Pollution Research, 1182 Sowa, Nishi-ku, Niigata, Niigata, 950-2144, Japan
[4]Department of Advanced Technology Fusion, Konkuk University, Seoul, Korea
[5]Energy Systems Division, Argonne National Laboratory, Argonne, IL, USA
[6]National Institute for Environmental Studies, 16-2 Onogawa, Tsukuba, Ibaraki, 305-8506, Japan
[7]State Key Joint Laboratory of Environmental Simulation and Pollution Control, Department of Environmental Science, Peking University, Beijing, China
[8]Center for Global and Regional Environmental Research, University of Iowa, Iowa City, IA 52242, USA
[9]Multiphase Chemistry Department, Max Planck Institute for Chemistry, Mainz, Germany
[10]Institute of Energy, Environment and Economy, Tsinghua University, Beijing, China
[11]State Environmental Protection Key Laboratory of Sources and Control of Air Pollution Complex, Beijing, China
[12]Collaborative Innovation Center for Regional Environmental Quality, Beijing, China

Correspondence to: Qiang Zhang (qiangzhang@tsinghua.edu.cn)

Abstract. The MIX inventory is developed for the years 2008 and 2010 to support the Model Inter-Comparison Study for Asia (MICS-Asia) and the Task Force on Hemispheric Transport of Air Pollution (TF HTAP) by a mosaic of up-to-date regional emission inventories. Emissions are estimated for all major anthropogenic sources in 29 countries and regions in Asia. We conducted detailed comparisons of different regional emission inventories and incorporated the best available ones for each region into the mosaic inventory at a uniform spatial and temporal resolution. Emissions are aggregated to five anthropogenic sectors: power, industry, residential, transportation, and agriculture. We estimate the total Asian emissions of 10 species in 2010 as follows: 51.3 Tg SO_2, 52.1 Tg NO_x, 336.6 Tg CO, 67.0 Tg NMVOC (non-methane volatile organic compounds), 28.8 Tg NH_3, 31.7 Tg PM_{10}, 22.7 Tg $PM_{2.5}$, 3.5 Tg BC, 8.3 Tg OC, and 17.3 Pg CO_2. Emissions from China and India dominate the emissions of Asia for most of the species. We also estimated Asian emissions in 2006 using the same methodology of MIX. The relative change rates of Asian emissions for the period of 2006–2010 are estimated as follows: −8.1 % for SO_2, +19.2 % for NO_x, +3.9 % for CO, +15.5 % for NMVOC, +1.7 % for NH_3, −3.4 % for PM_{10}, −1.6 % for $PM_{2.5}$, +5.5 % for BC, +1.8 % for OC, and +19.9 % for CO_2. Model-ready speciated NMVOC emissions for SAPRC-99 and CB05 mechanisms were developed following a profile-assignment approach. Monthly gridded emissions at a spatial resolution of $0.25° \times 0.25°$ are developed and can be accessed from http://www.meicmodel.org/dataset-mix.

1 Introduction

The Model Inter-Comparison Study for Asia (MICS-Asia) project is currently in phase III. During the previous two phases, studies have been focused on long-range transport and deposition of pollutants, global inflow of pollutants to Asia, model sensitivities to aerosol parameterization, and emissions over Asia (Carmichael et al., 2002, 2008; Han et al., 2008; Hayami et al., 2008; Holloway et al., 2008; Wang et al., 2008). MICS-Asia Phase III aims to conduct further inter-comparisons of atmospheric modeling for Asia and analyze the disagreement of model output and relative uncertainties. In this regard, common meteorological fields, emission data, and boundary conditions should be used. One of the key tasks in MICS-Asia Phase III is to develop a reliable Asian emission inventory as common input for model intercomparisons through integration of state-of-the-art knowledge on Asian emissions.

A reasonable understanding of anthropogenic emissions is essential for atmospheric chemistry and climate research (Xing et al., 2013; Keller et al., 2014). Hence, the community has put tremendous efforts into developing better emission inventories (Granier et al., 2011). For a large geographic region like Asia, compiling a bottom-up emission inventory is a challenging task because it requires a huge amount of local information on energy use, technologies, and environmental regulations for many different countries.

Generally, there are two common approaches to develop a bottom-up emission inventory at regional level. One is using a unified framework of source categories, calculating method, chemical speciation scheme (if applicable), and spatial and temporal allocations (e.g., Streets et al., 2003; Ohara et al., 2007; Lu et al., 2011). Using the unified approach, emissions are estimated in a consistent way with attainable resources. Several Asian emission inventories widely used in the community were developed by the unified approach. Streets et al. (2003) first developed a comprehensive Asian emission inventory for a variety of gaseous and aerosol species for the year 2000 to support the TRACE-P (Transport and Chemical Evolution over the Pacific) campaign (Carmichael et al., 2003), which was subsequently used for MICS-Asia Phase II. Ohara et al. (2007) developed the Regional Emission inventory in Asia (REAS) version 1.1 covering emissions of major species over Asia from 1980 to 2003, which provides estimates of Asian emissions for a long-term period. However, with the unified approach, many region-dependent parameters are shared among different regions due to lack of resources and local knowledge (e.g., emission factors, chemical profiles, spatial proxies, and temporal profiles, etc.), introducing large uncertainties in emission estimates for a specific region (He et al., 2007; Kurokawa et al., 2009).

The other is the "mosaic" approach that harmonizes various emission inventories of different regions into one emission data product at large scale, by normalization of source categories, species, and spatial and temporal resolution from different inventories and providing emission data with uniform format. Available emission inventories always differ in geographic region, time period, source classification, species, and spatial and temporal resolution, introducing complexities in intercomparisons of emissions and model results with different emission inputs. By involving the state-of-the-art local emission inventories developed with local knowledge and harmonizing them to uniform format, this approach can provide a reference on magnitude and spatial distribution of emissions for different regions, while there is always trade-off in spatial–temporal coverage and resolution due to inconsistencies among involved inventories.

Recent studies (e.g., Zhang et al., 2009; Kurokawa et al., 2013) tend to use the mosaic approach to supplement the Asian emission inventory developments. To support the NASA's INTEX-B (the Intercontinental Chemical Transport Experiment Phase B) mission (van Donkelaar et al., 2008; Adhikary et al., 2010), Zhang et al. (2009) developed a new emission inventory for Asia for the year 2006 as an update and improvement of the TRACE-P inventory (Streets et al., 2003). Compared to the TRACE-P inventory, the INTEX-B inventory improved emission estimates for China by introducing a technology-based methodology and incorporated several local inventories including BC and OC emissions for India from Reddy et al. (2002a, b), a Japan emission inventory from Kannari et al. (2007), and official emission inventories for the Republic of Korea and Taiwan. In the updated version 2.1 of the REAS inventory (Kurokawa et al., 2013), a few regional inventories developed with local knowledge are also incorporated to improve the accuracy (see Sect. 2.2.1 for details).

In order to support the MICS-Asia III and other global and regional modeling activities with the best available anthropogenic emission dataset over Asia, we develop a new Asian anthropogenic emission inventory, named MIX, by harmonizing different local emission inventories with the mosaic approach. The mosaic inventory developed in this work will provide (1) a more complete and state-of-the-art understanding of anthropogenic emissions over Asia with best estimates from local inventories; (2) a reference dataset with moderate accuracy and resolution that can support both scientific research and mitigation policy-making; and (3) broader application of the best available local inventories in modeling studies by processing them to model-ready format and including them in a publicly available emission dataset.

The MIX inventory is developed for 2008 and 2010, in accordance with base year simulations in MICS-Asia III and the Task Force on Hemispheric Transport of Air Pollution (TF HTAP). It should be noted that MIX is not comparable to INTEX-B and TRACE-P to derive an emission trend due to differences in methodology and underlying data. In this paper, we also provided Asian emissions for 2006 using the same methodology, partly resolving the problems of trend analysis in mosaic inventories. The gridded MIX emission data for the years 2008 and 2010 are then incorporated
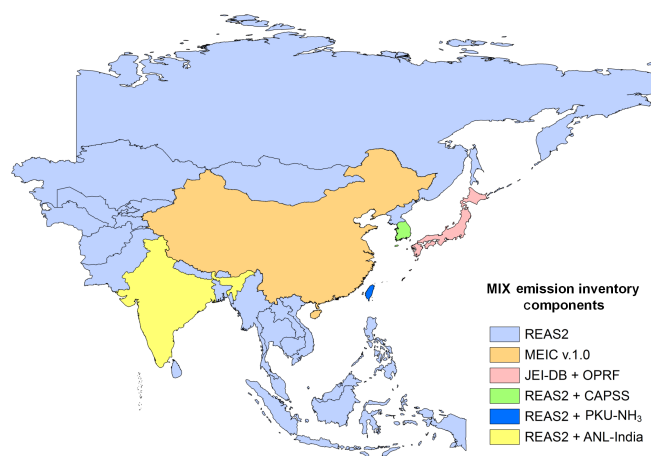
Figure 1. Domain and component of the MIX emission inventory.

into the HTAP v2.2 global emission inventory (Janssens-Maenhout et al., 2015) to support the modeling activities in HTAP, providing a consistent emission input for global and regional modeling activities.

Figure 1 presents the definition of the MIX domain and emission datasets used for each country and region. The domain of MIX covers 29 countries and regions (the full list of country and region names are listed in Table 1), stretching from Kazakhstan in the west to Russia Far East in the east and from Indonesia in the south to Siberia in the north. Emissions are aggregated into five sectors: power, industry, residential, transportation, and agriculture. Ten chemical species are included in the MIX inventory, including both gaseous and aerosol species: SO_2, NO_x, CO, NMVOC (non-methane volatile organic compounds), NH_3 (ammonia), PM_{10} (particulate matter with diameter less than or equal to 10 μm), $PM_{2.5}$ (particulate matter with diameter less than or equal to 2.5 μm), BC (black carbon), OC (organic carbon), and CO_2. Only emissions from anthropogenic sources are included in MIX. NMVOC emissions are speciated into model-ready inputs for two chemical mechanisms: CB05 (the Carbon Bond mechanism; Yarwood et al., 2005) and SAPRC-99 (the State Air Pollution Research Center 1999 version; Carter, 2000) (see Tables S1 and S2 in the Supplement). Monthly emissions are provided by sector at $0.25° \times 0.25°$ resolution. Gridded emissions are available from http://www.meicmodel.org/dataset-mix. The key features of the MIX inventory are summarized in Table 1.

This paper documents the methodology and emission datasets of the MIX Asian anthropogenic emission inventory. The regional and national inventories used to develop MIX gridded datasets and the mosaic methodology are presented in Sect. 2. Section 3 presents Asian emissions in 2010 and spatial and temporal variations in emissions. Changes in Asian emissions between 2006 and 2010 are also discussed. Section 4 highlights the major improvements in the new inventory by comparing MIX with other Asian emission in-

ventories. Uncertainties and limitations of the inventory are discussed in Sect. 5. Concluding remarks are provided in Sect. 6.

2 Compilation of the MIX emission inventory

2.1 Methodology

Five emission inventories are collected and incorporated into the mosaic inventory, as listed in the following: REAS inventory version 2.1 for the whole of Asia (referred to as REAS2 hereafter; Kurokawa et al., 2013), the Multi-resolution Emission Inventory for China (MEIC) developed by Tsinghua University (http://www.meicmodel.org), a high-resolution NH_3 emission inventory by Peking University (referred to as PKU-NH_3 inventory hereafter; Huang et al., 2012), an Indian emission inventory developed by Argonne National Laboratory (referred to as ANL-India hereafter; Lu et al., 2011; Lu and Streets, 2012), and the official Korean emission inventory from the Clean Air Policy Support System (CAPSS; Lee et al., 2011).

We then selected different emission datasets for various species for each country by the following hierarchy. REAS2 was used as the default where local emission data are absent. Emission inventories compiled by the official agencies or developed with more local information are selected to override REAS2, which include MEIC for mainland China, ANL-India for India, and CAPSS for the Republic of Korea. Detailed information and advantages of these inventories are presented in Sect. 2.2. As only a few species (SO_2, BC, OC, and power plant NO_x) were available from ANL-India, REAS2 was used to supplement the missing species. A mosaic process was then used to combine ANL-India and REAS2 into a single dataset for Indian emissions. It is worth noting that the REAS2 has incorporated local inventories for Japan and Taiwan, which are subsequently adopted in MIX for these two regions. PKU-NH_3 was further used to replace MEIC emissions for NH_3 over China, given that PKU-NH_3 was developed with a process-based model that represented the spatiotemporal variations in NH_3 emissions. Table 2 lists the information of each inventory used in MIX.

Figure 2 illustrates the mosaic process for the MIX inventory development. Each dataset was reprocessed to $0.25° \times 0.25°$ resolution with monthly variations when necessary. We used monthly gridded emissions from each component inventory where available and assumed no monthly variation in emissions when the component inventory only provided annual emissions. The monthly profiles and spatial proxies used in each component emission inventories are summarized in Tables S3 and S4.

For each regional emission inventory, emissions were acquired with subsector information and then aggregated into five sectors: power, industry, residential, transportation, and agriculture. Table S5 presented the sectoral mapping tables

Table 1. Summary of the MIX Asian anthropogenic emission inventory.

Item	Description
Domain	29 countries and regions in Asia
Countries and regions	China, Japan, Democratic People's Republic of Korea, Republic of Korea, Mongolia, India, Afghanistan, Bangladesh, Bhutan, Maldives, Nepal, Pakistan, Sri Lanka, Brunei, Cambodia, Indonesia, Laos, Malaysia, Myanmar, Philippines, Singapore, Thailand, Vietnam, Kazakhstan, Kyrgyzstan, Tajikistan, Turkmenistan, Uzbekistan, Russia (East Siberia, Far East, Ural, West Siberia)
Species	SO_2, NO_x, CO, NMVOC, NH_3, PM_{10}, $PM_{2.5}$, BC, OC, CO_2
VOC speciation	by chemical mechanisms: CB05, SAPRC-99
Sectors	power, industry, residential, transportation, agriculture
Spatial resolution	$0.25° \times 0.25°$
Seasonality	monthly
Year	2008, 2010
Data Access	http://www.meicmodel.org/dataset-mix

Table 2. List of regional emission inventories used in this work.

	MEIC v1.0	PKU-NH$_3$	CAPSS	JEI-DB+OPRF	ANL-India		REAS2
Year	1990–2010	2006	2008, 2010	2008, 2010	1996–2010	2008, 2010	2000–2010
Region	China	China	Republic of Korea	Japan	India	India	Asia
Seasonality	Monthly	Monthly	Annual	Monthly	Monthly	Annual	Monthly
Resolution	0.25°*	1 km	0.25°	1 km	0.1°	0.25°*	0.25°*
SO_2	X		X	X	X		X
NO_x	X		X	X		X	X
CO	X		X	X			X
NMVOC	X		X	X			X
NH_3	X	X		X			X
PM_{10}	X		X	X			X
$PM_{2.5}$	X			X			X
BC	X			X	X		X
OC	X			X	X		X
CO_2	X		X	X			X
NMVOC speciation	X						X

* Power plant emissions are developed with specific geophysical locations and allocated into $0.25° \times 0.25°$ grids.
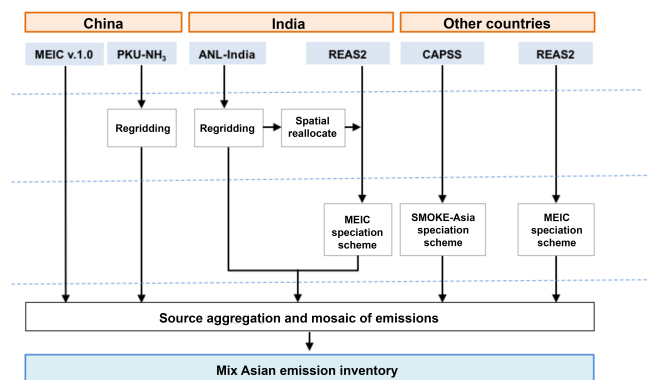
Figure 2. Schematic methodology of the MIX emission inventory development.

from subsectors to the five MIX sectors for each regional inventory. For each subsector, the corresponding IPCC sectors are also provided in Table S5. For agriculture sector, only NH_3 emissions are provided in the MIX inventory given that soil NO_x emissions and agriculture PM emissions are not available in the regional inventories used for compiling MIX. Emissions from open biomass burning, fugitive dust, aviation, and international shipping were excluded in the MIX inventory because those emissions were only available in a few inventories.

NMVOC emissions were speciated to SAPRC-99 and CB05 mechanisms following the explicit species mapping approach documented in Li et al. (2014) (see Fig. 3). Finally, emissions were aggregated to the five MIX sectors and then assembled to monthly emission grid maps over Asia with a uniform spatial resolution of $0.25° \times 0.25°$.
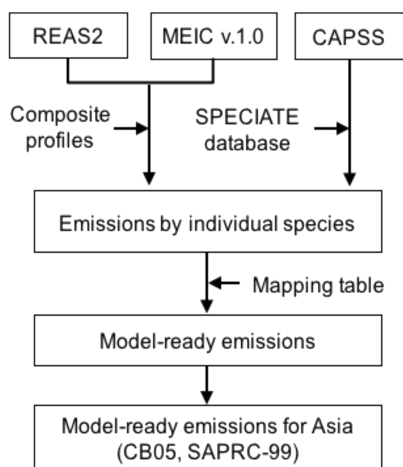
Figure 3. NMVOC speciation scheme used in the MIX inventory development. The mapping table is derived from Carter (2013).

2.2 Components of the MIX emission inventory

2.2.1 REAS2

We used anthropogenic emissions from REAS2 (Kurokawa et al., 2013) to fill the gap where local emission data are not available. REAS2 updated the REAS version 1.1 for both activity data and emission factors by each country and region using global and regional statistics and recent regional specific studies on emissions factors. Improved from its previous version, power plant emissions in REAS2 were estimated by combining information on generation capacity, fuel type, running years, and CO_2 emissions from the Carbon Monitoring for Action database (CARMA; Wheeler and Ummel, 2008) and the World Electric Power Plants database (WEPP; Platts, 2009). REAS2 extended the domain to include emissions of Central Asia and the Asian part of Russia (referred to as Russia Asia). Readers can refer to Kurokawa et al. (2013) for detailed data sources of activity rates and emission factors assignments for each country and source type. REAS2 is available for the period of 2000–2008. In this work, we updated the REAS2 to the year 2010, following the same approach documented in Kurokawa et al. (2013).

REAS2 also incorporated a few regional inventories developed by local agencies with detailed activity data and emission factors, including the JEI-DB inventory (Japan Auto-Oil Program (JATOP) Emission Inventory-Data Base; JPEC, 2012a, b, c) for all anthropogenic sources in Japan excluding shipping, OPRF (Ocean Policy Research Foundation; OPRF, 2012) for shipping emissions in Japan, CAPSS emission inventory for Korea (Lee et al., 2011), and official emission data from the Environmental Protection Administration of Taiwan for Taiwan (Kurokawa et al., 2013). All these regional datasets were then harmonized to the same spatial and temporal resolution in REAS2. In this work, we processed the CAPSS emission data separately as an individual data source, which is presented in Sect. 2.2.5, and adopted Japan and Taiwan emissions directly from the REAS2 product.

The REAS2 inventory is provided with monthly gridded emission data for both air pollutants and CO_2 by sectors at $0.25 \times 0.25°$ resolution. We aggregated the 11 REAS2 sectors to 5 sectors provided in the MIX inventory. Emissions from open biomass burning, aviation, and international shipping were excluded from the REAS2 before incorporating into MIX. Monthly variations are developed for power plants, industry, residential sources, and cold-start emissions from vehicles by various monthly profiles (Kurokawa et al., 2013). In REAS2, power plants with annual CO_2 emissions larger than 1 Tg were provided as point sources with coordinates of locations, while emissions for other sectors were processed as areal sources and gridded at $0.25 \times 0.25°$ resolution using maps of rural, urban, and total populations and road networks (see Table S4).

2.2.2 MEIC

We use anthropogenic emission data generated from the MEIC (Multi-resolution Emission Inventory for China) model to override emissions in mainland China. MEIC is a bottom-up emission inventory framework developed and maintained by Tsinghua University, which uses a technology-based methodology to calculate air pollutant and CO_2 emissions for more than 700 anthropogenic emitting sources for China from 1990 to the present. With the detailed source classification, the MEIC model can represent emission characteristics from different sectors, fuels, products, combustion/process technologies, and emission control technologies. The MEIC model improved the bottom-up emission inventories developed by the same group (Streets et al., 2006; Zhang et al., 2007a, b, 2009; Lei et al., 2011) and integrated them into a uniform framework. The major improvements include a unit-based power plant emission database (Wang et al., 2012; Liu et al., 2015), a high-resolution vehicle emission modeling approach (Zheng et al., 2014), an explicit NMVOC speciation assignment methodology (Li et al., 2014), and a unified, online framework for emission calculation, data processing, and data downloading (available at http://www.meicmodel.org).

Power plant emissions in MEIC were derived from the China coal-fired Power plant Emissions Database (CPED), in which emissions were estimated for each generation unit based on the unit-specific parameters including fuel consumption rates, fuel quality, combustion technology, and emission control technology. With detailed information of over 7600 generation units in China, CPED improved the spatial and temporal resolution of the power plant emission inventory compared to previous studies (Liu et al., 2015). For the on-road transportation sector, MEIC used the new approach developed by Zheng et al. (2014), which estimated vehicle emissions with high spatial resolution by using vehicle population and emission factors at county level. County-

level emissions were further allocated to high-resolution grids based on a digital road map and weighting factors of vehicle kilometers traveled by vehicle and road type.

MEIC provides lumped speciated NMVOC emissions for different chemical mechanisms, e.g., SAPRC-99, SAPRC-07, CBIV, CB05, and RADM2. Following the speciation assignment approach developed by Li et al. (2014), emissions of individual NMVOC species were calculated for each source category by splitting the total NMVOC emissions with corresponding source profiles. Emissions were then assigned to various mechanisms using species mapping tables.

MEIC delivers monthly emissions at various spatial resolutions through an open-access, online framework (http://www.meicmodel.org). Monthly variations and gridded emissions were generated by sector using different temporal profiles and spatial proxies. Users can define the metadata (species, domain range, time period, sectors, spatial resolution, and chemical mechanisms), calculate gridded emissions, and download data from the website. Monthly emissions at $0.25° \times 0.25°$ generated from MEIC v1.0 (referred to as MEIC hereafter) were used in MIX. Emissions were aggregated to four MIX sectors: power, industry, residential, and transportation. NH_3 emissions in MEIC were replaced by PKU-NH_3, which will be discussed in the next section.

2.2.3 PKU-NH$_3$ for China

We used a high-resolution NH_3 emission inventory in China compiled by Peking University (PKU-NH_3; Huang et al., 2012) to replace China's NH_3 emissions in MEIC. MEIC used annual and regional average NH_3 emission factors to calculate emissions from each source category, while PKU-NH_3 used a process-based model to estimate NH_3 emissions which parameterized the spatial and temporal variations of emission factors with consideration of ambient temperature, soil property, and other factors. For NH_3 emissions from fertilizer applications, fertilizer type, soil property, fertilizer application method, application rate, and ambient temperature were used to develop monthly and gridded emission factors. For livestock wastes, emissions were estimated based on a mass-flow methodology by tracing the migration and volatilization of nitrogen from each stage of livestock manure management.

PKU-NH_3 estimated NH_3 emissions in China (including mainland China and Hong Kong, Macao, and Taiwan) in 2006 for the following sources: livestock wastes, farmland ecosystem, biomass burning, excrement from rural population, chemical industry, waste disposal, and transportation. Open biomass burning was excluded from the MIX inventory aggregation since the MICS-Asia III project uses GFED dataset for biomass burning. PKU-NH_3 is available at $1 \, km \times 1 \, km$ resolution with monthly variation. We then regridded PKU-NH_3 monthly emissions to $0.25° \times 0.25°$. In the MIX inventory, 2006 emissions from PKU-NH_3 are used for both 2008 and 2010 since 2006 is the most recent year

for emissions in PKU-NH_3 when the MIX inventory was developed. As the major drivers of NH_3 emissions, synthetic fertilizer consumption and animal population increased by 4 and 9 % from 2006 to 2010, respectively, much smaller than the growth rates of coal consumption and vehicle population for the same period.

2.2.4 ANL emission inventories for India

A high-resolution Indian emission inventory developed by ANL (referred to as ANL-India hereafter; Lu et al., 2011) was used in the MIX inventory. ANL-India used a technology-based methodology to estimate SO_2, BC, and OC emissions in India for the period of 1996–2010. Major anthropogenic sources including both fossil-fuel and biofuel combustion are covered in ANL-India. Time-dependent trends in emission factors were developed by taking account of the impact of technology changes on emissions (Habib et al., 2004; Venkataraman et al., 2005). Lu and Streets (2012) further updated power plant emissions in India by calculating emissions at the generating unit level (~ 800 units in total) based on information from the reports of the Central Electricity Authority (CEA), including geographical location, capacity, fuel type, electricity generation, time the plant was commissioned/decommissioned, etc. The exact location of each power plant was obtained from the Global Energy Observatory (http://globalenergyobservatory.org) and crosschecked through Google Earth. The updated unit-based power plant emissions in ANL-India are available for SO_2, NO_x, BC, and OC.

ANL-India is available for the period of 1990–2010 at $0.1° \times 0.1°$ resolution with monthly variations. Emissions are presented by sectors, i.e., power, industry, residential, transportation, and open biomass burning. Monthly variations in ANL-India were developed by sector using various surrogates (Lu et al., 2011). As ANL-India only covers some of the required MIX species (SO_2, BC, and OC for all sectors, NO_x for power plants), monthly emissions by sector (excluding open biomass burning) from ANL-India were first regridded to $0.25° \times 0.25°$ and then merged with REAS2 before being implemented in MIX to cover all species. The merge process is presented in Sect. 2.3.

2.2.5 CAPSS inventory for the Republic of Korea

For the Republic of Korea, we used the CAPSS emission inventory developed by the National Institute of Environmental Research of Korea (Lee et al., 2011). CAPSS estimated emissions with four levels of source classifications. We mapped emissions from 12 first-level aggregated source categories (SCC1) to five sectors in MIX. The CAPSS inventory included emissions for CO_2 and five regulated air pollutants, SO_2, NO_x, CO, NMVOC, and PM_{10}. We derived sector-specific emission ratios between PM_{10} and the other aerosol components from Lei et al. (2011) and applied those

ratios to estimate $PM_{2.5}$, BC, and OC emissions. In the MIX inventory, we used the 2008 and 2009 CAPSS inventories to represent 2008 and 2010 emissions of the Republic of Korea, because 2009 is the most recent year of CAPSS inventory at the time the MIX inventory was developed. In the CAPSS inventory, point sources, area sources, and mobile sources were processed using different spatial allocation approaches (Lee et al., 2011). We used the $0.25° \times 0.25°$ emission product from CAPSS as input for the MIX inventory. Only annual total emissions were presented in the CAPSS inventory. In the MIX inventory, we assume no monthly variation in emissions in the Republic of Korea.

2.3 Mosaic of Indian emission inventory

ANL-India is available for SO_2, BC, and OC for all sectors as well as NO_x for power plants. In this work, REAS2 is used to supplement the missing species in ANL-India. To reduce possible inconsistencies from implementation of the two different inventories, we have reprocessed ANL-India and REAS2 emissions over India in the following two steps.

First, for power plants, because ANL-India used CEA reports to derive information of individual power generation units while REAS2 used the CARMA and WEPP databases to get similar information, direct merging of the two products could introduce inconsistency due to a mismatch of unit information in the two databases. In this work, we directly used ANL-India for SO_2, NO_x, BC, and OC emissions and used REAS2 for CO, NMVOC, $PM_{2.5}$, PM_{10}, and CO_2 but redistributed the total magnitudes of REAS2 power plant emissions by using the spatial distribution of power plants in the ANL-India inventory. We generated the spatial proxies of fuel consumption for each fuel type (coal, oil, and gas) at $0.25 \times 0.25°$ by aggregating fuel consumptions of each unit in the ANL-India inventory. We then applied the spatial proxy to the REAS2 estimates by fuel type for species that were not included in ANL-India.

Second, we used BC and OC emissions from ANL-India but used $PM_{2.5}$ and PM_{10} emissions from REAS2. In certain grids, the sum of BC and OC emissions may exceed $PM_{2.5}$ emissions because the two inventories may use different activity data, emission factors, and spatial proxies. The so-called "PMfine" species in chemical transport models are usually calculated by subtracting BC and OC emissions from total $PM_{2.5}$ emissions, leading to negative emissions of PMfine in those grids. In this case, we adjusted the emissions of $PM_{2.5}$ to the sum of BC and OC emissions for each sector.

2.4 NMVOC speciation of the MIX inventory

In the MIX inventory, we provide model-ready speciated NMVOC emissions over Asia (except the Republic of Korea) for both CB05 and SAPRC-99 chemical mechanisms, by using the explicit species mapping approach and updated NMVOC profiles developed in Li et al. (2014), as illustrated

in Fig. 3. Following Li et al. (2014), NMVOC emissions for CB05 and SAPRC-99 species are calculated as follows:

$$\text{EVOC}(i,k,m) = \sum_{j=1}^{n} \left[\frac{\text{EVOC}(i,k) \times X(i,j)}{\text{mol}(j)} \times C(j,m) \right], \quad (1)$$

where k is the region, m is species type in CB05 or SAPRC-99 mechanisms, and n is the number of species emitted from source i. EVOC is the total NMVOC emissions by source type. In this work, emissions in China and other Asian countries were derived from MEIC and REAS2 respectively. $X(i,j)$ is the mass fraction of species j in the total NMVOC emissions for source i, which is taken from the profiles developed by Li et al. (2014). Those profiles were constructed by grouping and averaging multiple profiles from both local measurements and the SPECIATE database (Hsu and Divita, 2009; Simon et al., 2010). Mol(j) is the mole weight of species j and $C(j,m)$ is the conversion factor between j and m obtained from the mapping tables in Carter (2013).

For the Republic of Korea, the SMOKE-Asia model developed by Woo et al. (2012) was used to calculate model-ready NMVOC emissions for both CB05 and SAPRC-99 mechanisms. NMVOC emissions from the CAPSS were mapped to Source Classification Codes (SCCs) and country–state–county (FIPS) code in SMOKE-Asia model and speciated NMVOC emissions were then calculated by linking emissions to speciation profiles with cross references.

2.5 Monthly profiles

We directly used monthly emissions from each regional emission inventory when compiling the MIX inventory. We assume no monthly variation in emissions when monthly profiles are absent from the regional emission inventories. Table S3 presents the monthly profiles used in each component emission inventory for MIX. In summary, monthly profiles for power plant emissions usually developed based on monthly statistics of power generation. Monthly profiles of industrial emissions are derived from monthly output of industrial products or industrial GDP. Residential monthly profiles are estimated from stove operation time based on ambient temperatures by regions (Streets et al., 2003).

2.6 Spatial proxies

We used gridded emissions from each regional emission inventory to compile the grid maps of emissions. Locations of emitting facilities were used to derive gridded emission for large sources, while spatial proxies such as population density, road networks, and land use information are used to allocate emissions of areal sources. Table S4 summarized spatial proxies used in developing gridded emissions for each regional inventory.
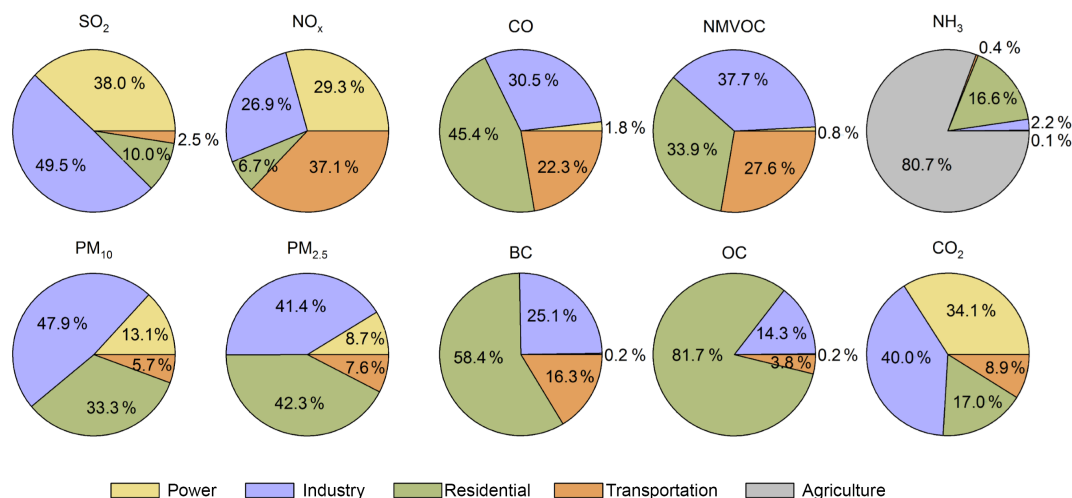
Figure 4. Emission distributions among sectors in Asia in 2010.

3 Results

3.1 Asian anthropogenic emissions in 2010

Based on the mosaic approach and candidate inventories described in Sect. 2, gridded anthropogenic emissions for 10 species were generated over Asia and called the MIX emission inventory. In the MIX inventory, Asian anthropogenic emissions in 2010 are estimated as follows: 51.3 Tg SO_2, 52.1 Tg NO_x, 336.6 Tg CO, 67.0 Tg NMVOC, 28.8 Tg NH_3, 31.7 Tg PM_{10}, 22.7 Tg $PM_{2.5}$, 3.5 Tg BC, 8.3 Tg OC, and 17.3 Pg CO_2. Figure 4 presents the emission distributions among sectors over Asia in 2010. Among the different sectors, the industrial sector has the largest contribution to SO_2 (50 % of total), NMVOC (38 %), PM_{10} (48 %), and CO_2 (40 %) emissions. Power plants have significant contributions for SO_2 (38 % of total), NO_x (29 %), and CO_2 (34 %) emissions.

Asian emissions in 2010 for 10 species are listed in Table 3 by country and the shares of 2010 emissions by each subregion are presented in Fig. 5. China is the largest contributor for most species except NH_3, with more than 50 % contribution for SO_2, NO_x, CO, PM_{10}, $PM_{2.5}$, and CO_2 emissions. Following China, India is the largest contributor for NH_3 emissions (34 % of total) and the second largest contributor for all other species. As shown in Fig. 5, Southeast Asia and Other South Asia contribute more than 20 % to NMVOC, NH_3, OC, and CO emissions and around 10 % for other species, representing, in particular, a high contribution from biofuel emissions. Contributions from other Asian regions are less than 10 % for all species.

Table 4 presents Asian 2010 emissions by region and by sector. Emissions by country and by sector can be downloaded from the MIX website (http://www.meicmodel.org/dataset-mix.html). China's anthropogenic emissions in 2010 are estimated as follows: 28.7 Tg SO_2, 29.1 Tg NO_x, 170.9 Tg CO, 23.6 Tg NMVOC, 9.8 Tg NH_3, 16.6 Tg PM_{10}, 12.2 Tg $PM_{2.5}$, 1.8 Tg BC, 3.4 Tg OC, and 10.1 Pg CO_2. Overall, industry is the largest emitter of China's anthropogenic emissions, contributing 49 % of the total CO_2 emissions and 59, 39, 61, and 50 % of SO_2, NO_x, NMVOC, and $PM_{2.5}$ emissions respectively. The dominance of the industrial sector on China's anthropogenic emissions reflects the fact that China has developed a huge industrial capacity, which has led to very high levels of energy use and emissions. For example, China produced 44 and 70 % of global iron and cement, respectively, in 2010 (World Steel Association, 2011; United Nations, 2011). As a result, industrial SO_2 emissions in China in 2010 surpassed SO_2 emissions from the US and Europe combined. Power plants contributed 32 % of the total CO_2 emissions and 28, 33, and 7 % of SO_2, NO_x, and $PM_{2.5}$ emissions respectively. Emission ratios of SO_2 / CO_2 and $PM_{2.5}$ / CO_2 are lower in power plants than in the industrial sector, reflecting better emission control facilities operated in power plants, such as flue-gas desulfurization devices (FGD). The residential sector dominates emissions for pollutants from incomplete combustion, given that large amounts of solid fuels (coal and biomass) were burned in small stoves in China's homes. The residential sector shared 13 % of China's total CO_2 emissions in 2010, but contributed to 45 % of CO, 27 % of NMVOC, 51 % of BC, and 81 % of OC emissions respectively. The transportation sector accounted for 25, 12, 11, and 16 % of NO_x, CO, NMVOC, and BC emissions respectively. The contribution of the transportation sector to China's CO and NMVOC emissions has substantially decreased during recent years, which will be further discussed in the next section.

In the MIX inventory, Indian emissions in 2010 are estimated as follows: 9.3 Tg SO_2, 9.6 Tg NO_x, 67.4 Tg CO, 16.9 Tg NMVOC, 9.9 Tg NH_3, 7.1 Tg PM_{10}, 5.2 Tg $PM_{2.5}$, 1.0 Tg BC, 2.5 Tg OC, and 2.3 Pg CO_2. In India, the indus-

Table 3. National anthropogenic emissions in the MIX emission inventory in 2010 (units: Tg for CO_2 and Gg for other species). Bold values are the total emissions for Asian regions.

Countries	SO_2	NO_x	CO	NMVOC	NH_3	PM_{10}	$PM_{2.5}$	BC	OC	CO_2
China[a]	**28 663**	**29 071**	**170 874**	**23 619**	**9804**	**16 615**	**12 200**	**1765**	**3386**	**10 124**
Japan	708	1914	4278	1178	479	114	81	20	8	1107
Korea, DPR	211	238	4488	138	111	264	115	14	17	71
Korea, Republic of	418	1062	838	851	190	124	87	24	8	541
Mongolia	99	62	735	47	97	109	46	2	4	15
Other East Asia[b]	**1437**	**3275**	**10 339**	**2215**	**875**	**610**	**328**	**60**	**37**	**1735**
India	**9259**	**9565**	**67 423**	**16 892**	**9871**	**7093**	**5216**	**1019**	**2530**	**2277**
Afghanistan	3	178	456	141	143	21	20	8	10	2
Bangladesh	133	368	2575	788	1016	342	234	33	121	84
Bhutan	5	13	302	50	41	26	21	4	14	5
Maldives	3	8	151	9	1	0	0	0	0	2
Nepal	30	83	2109	443	254	150	139	27	105	34
Pakistan	1397	946	9279	2112	1859	600	558	114	390	263
Sri Lanka	133	116	1321	367	122	152	111	15	59	31
Other South Asia[b]	**1704**	**1712**	**16 194**	**3910**	**3435**	**1290**	**1082**	**200**	**699**	**421**
Brunei	11	12	6	32	8	1	0	0	0	9
Cambodia	26	47	1025	211	134	59	56	11	44	17
Indonesia	1964	2570	23 749	7970	1945	1182	947	178	692	554
Laos	150	41	397	85	87	24	22	4	16	6
Malaysia	365	631	3731	1765	255	216	132	16	35	201
Myanmar	67	91	2705	814	425	165	156	31	125	49
Philippines	503	361	2347	869	413	193	123	15	68	119
Singapore	175	116	162	334	10	7	5	1	1	43
Thailand	614	809	8572	2327	649	495	275	35	149	297
Vietnam	575	442	8231	2234	665	710	562	87	322	232
Southeast Asia[b]	**4449**	**5120**	**50 925**	**16 640**	**4592**	**3051**	**2278**	**378**	**1452**	**1527**
Kazakhstan	1050	559	3348	544	41	442	222	13	28	204
Kyrgyzstan	27	35	371	40	12	62	28	2	3	6
Tajikistan	14	25	192	30	15	22	13	1	1	4
Turkmenistan	64	124	417	238	14	64	30	2	3	52
Uzbekistan	493	228	899	310	50	373	165	3	11	121
Central Asia[b]	**1648**	**971**	**5227**	**1162**	**133**	**963**	**458**	**21**	**46**	**387**
East Siberia	1649	534	2874	394	23	368	198	14	20	184
Far East	358	489	2681	303	18	223	123	22	25	120
Ural	1480	456	4005	591	22	1047	598	19	75	186
West Siberia	677	926	6045	1310	42	465	269	32	52	340
Russia Asia[b]	**4164**	**2405**	**15 605**	**2597**	**105**	**2103**	**1188**	**87**	**172**	**830**
Asia	**51 324**	**52 118**	**336 588**	**67 034**	**28 816**	**31 726**	**22 749**	**3530**	**8322**	**17 301**

[a] Hong Kong, Macao, and Taiwan are included. [b] The Asian region includes the set of countries listed in the section.

trial sector has much lower contributions to emissions compared to China, while higher emission contributions from the residential sector are estimated. The differences of the emission patterns between China and India can be attributed to differences in the stage of economic development and the composition of the energy structure. In India, the residential sector is the second largest contributor for CO_2 emissions and the largest contributor for CO, NMVOC, $PM_{2.5}$, BC, and OC emissions, in which more than 70 % of those emissions are contributed by biofuel combustion. With the rapid growth

Table 4. Asian emissions by sector in 2010 for each region (units: Tg for CO_2 and Gg for other species). Bold values are the total emissions for Asian regions.

| Regions	SO_2	NO_x	CO	NMVOC	NH_3	PM_{10}	$PM_{2.5}$	BC	OC	CO_2
China	**28 663**	**29 071**	**170 874**	**23 619**	**9804**	**16 615**	**12 200**	**1765**	**3386**	**10 124**
Power	8166	9455	2077	255	0	1389	893	2	0	3245
Industry	16 775	11 218	71 276	14 461	239	9451	6061	575	530	4928
Residential	3489	1140	76 579	6349	450	5246	4737	908	2752	1266
Transportation	234	7257	20 942	2553	76	529	509	281	104	684
Agriculture					9040					
Other East Asia	**1437**	**3275**	**10 339**	**2215**	**875**	**610**	**328**	**60**	**37**	**1735**
Power	427	460	70	13	3	162	64	0	0	617
Industry	644	649	3329	1475	26	285	142	20	6	584
Residential	189	361	1402	259	143	77	47	8	18	233
Transportation	176	1805	5538	467	23	87	74	32	13	300
Agriculture					680					
India	**9259**	**9565**	**67 423**	**16 892**	**9871**	**7093**	**5216**	**1019**	**2530**	**2277**
Power	5476	2391	2676	125	8	2029	842	1	3	886
Industry	2959	973	18 164	3372	172	1284	931	217	200	585
Residential	685	968	34 317	7311	2185	2946	2640	709	2275	659
Transportation	139	5233	12 267	6085	9	834	802	92	52	147
Agriculture					7496					
Other South Asia	**1704**	**1712**	**16 193**	**3910**	**3436**	**1290**	**1082**	**200**	**699**	**421**
Power	774	290	51	6	0	24	12	0	1	79
Industry	546	165	2536	635	38	400	231	18	75	93
Residential	153	395	12 148	2600	724	777	753	147	594	199
Transportation	231	863	1459	669	1	90	87	34	29	49
Agriculture					2673					
Southeast Asia	**4449**	**5120**	**50 925**	**16 640**	**4592**	**3051**	**2278**	**378**	**1452**	**1527**
Power	1596	1136	580	110	10	540	157	2	0	393
Industry	2101	748	4309	3182	133	902	566	28	245	450
Residential	364	396	26 804	5792	1139	1478	1430	286	1140	424
Transportation	388	2840	19 233	7556	15	131	126	63	66	260
Agriculture					3296					
Central Asia	**1648**	**971**	**5227**	**1162**	**133**	**963**	**458**	**21**	**46**	**387**
Power	1066	379	40	7	1	4	1	0	0	155
Industry	407	134	354	623	7	930	428	6	32	105
Residential	154	131	576	159	85	3	3	1	2	98
Transportation	20	327	4257	373	1	26	26	15	12	29
Agriculture					39					
Russia Asia	**4164**	**2405**	**15 605**	**2597**	**105**	**2103**	**1188**	**87**	**172**	**830**
Power	1981	1149	478	26	6	27	15	2	9	517
Industry	1996	179	2727	1520	14	1949	1050	21	103	180
Residential	101	87	1056	236	58	23	20	4	16	63
Transportation	86	990	11							
,344	815	2	105	103	59	44	71			
Agriculture					25					
Asia	**51 324**	**52 118**	**336 588**	**67 034**	**28 816**	**31 726**	**22 749**	**3530**	**8322**	**17 301**
Power	19 487	15 260	5972	543	28	4175	1984	7	13	5893
Industry	25 429	14 065	102 695	25 267	629	15 200	9409	884	1192	6925
Residential	5134	3478	152 882	22 707	4784	10 551	9630	2063	6798	2944
Transportation	1274	19 316	75 040	18 517	126	1800	1727	576	320	1540
Agriculture					23 249					
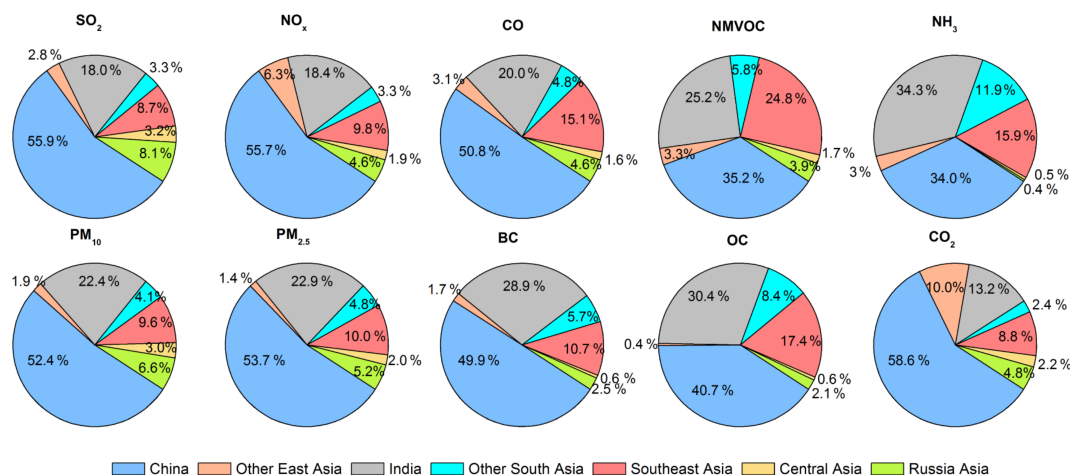
Figure 5. Emissions distributions by Asian regions in 2010.

of coal-fired generation units, SO_2 emissions from Indian power plants are estimated to be 5.5 Tg in 2010, contributing 59 % of the total Indian SO_2 emissions. The SO_2 / CO_2 emission ratio in Indian power plants is significantly higher than that of China, representing the low penetration rates of FGD in Indian power plants (Lu et al., 2011). The transportation sector contributes 55 % of NO_x and 36 % of NMVOC emissions in India. These large shares are caused by the high emission factors used in REAS2, in which relatively poor emission control measures are in place (Kurokawa et al., 2013).

Figure 6 compared per capita emissions by sector and by species in 2010 for each country. Emissions are ranked by GDP per capita of each country. The correlations between emission intensity (per capita emissions) and economic development (GDP per capita) at country level are not always significant because emission intensities are affected by not only economic level but also by other factors such as industrial structure and dominant fuel type. Nevertheless, the changes in emission intensities in general follow the pattern of Kuznets curve for most species except NH_3, BC, and OC. Emission intensities tend to increase following the GDP growth first and then tend to decrease for high-income countries. For BC and OC, per capita emissions are higher in developing countries than in developed countries because low-income countries with low incomes tend to use biofuels in which emitted more BC and OC than other fuel types.

Ratios of different species were widely used to inform emission characteristics. For example, SO_2 / CO_2 ratio was used as an indicator of coal combustion and emission control levels (Li et al., 2007), and ratios of CO / CO_2 were used to inform combustion efficiency (Wang et al., 2010). Figure 7 compares regional emission ratios of SO_2 / CO_2 and CO / CO_2 estimated by the MIX inventory. Emission ratios of SO_2 / CO_2 are lowest in Other East Asia among different regions, which could be attributed to small share of coal use

and high penetration of emission control facilities, while high emissions ratios of SO_2 / CO_2 were found in Russia Asia and Central Asia due to high fraction of coal use and less emission controls. Other East Asia also has the lowest emission ratios of CO / CO_2 among different regions, owing to a high contribution from industrial and transportation emissions. In contrast, high emissions from small residential combustions led to low combustion efficiencies and high emission ratio over India and Southeast Asia.

3.2 Changes of Asian emissions from 2006 to 2010

In this work, we also developed Asian emissions for 2006 and 2008 following the same approach of MIX, to illustrate the changes in Asian emissions from 2006 to 2010. Table 5 presents Asian emissions in 2006 and emission ratios of 2010 to 2016 by country. For the whole of Asia, emission growth rates from 2006 to 2010 are estimated as follows: −8.1 % for SO_2, +19.2 % for NO_x, +3.9 % for CO, +15.5 % for NMVOC, +1.7 % for NH_3, −3.4 % for PM_{10}, −1.6 % for $PM_{2.5}$, +5.5 % for BC, +1.8 % for OC, and +19.9 % for CO_2. Growth in CO_2 emissions represent the continuously increasing energy use across Asia during 2006–2010, while different trends among species represents differences in the emission control level among sectors and regions. Compared to the increasing emission trends of all species during 2001–2006 (Zhang et al., 2009), the relatively flat or even decreasing emission trends in many species indicate the effectiveness of emission control measures in recent years (Gu et al., 2013; Lin et al., 2010; Wang et al., 2013).

During 2006–2010, CO_2 emissions increased in China (+29.4 %), India (+20.4 %), Other South Asia (+15.2 %), and Southeast Asia (+12.3 %) and remained relatively stable for other regions. The increases in CO_2 emissions are driven by energy consumption growth stimulated by economic development over Asian regions, especially for China and India. As reported by IEA (International Energy Agency), the
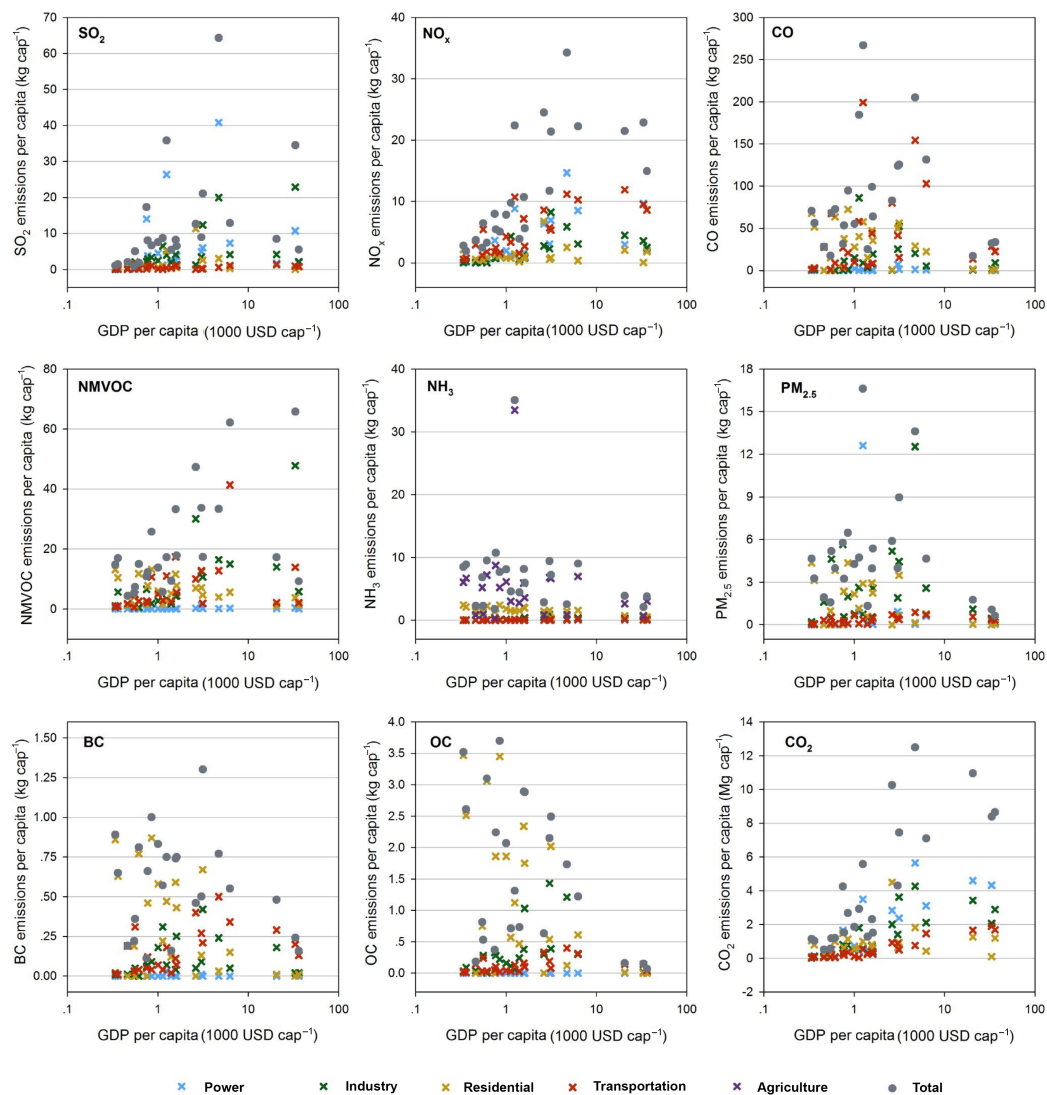
Figure 6. Per capita emissions by sector for 2010 in MIX, ranked by GDP per capita for each country.
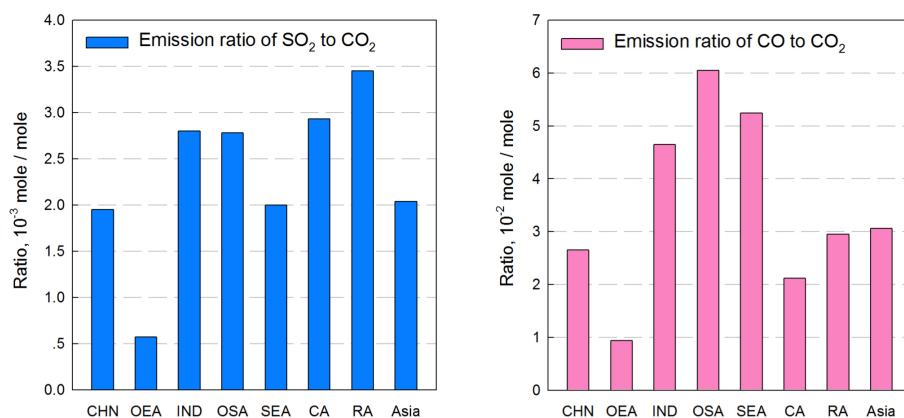

Figure 7. Emission ratios of SO_2 to CO_2, and CO to CO_2 by Asian regions. CHN is China, OEA is Other East Asia, IND is India, OSA is Other South Asia, SEA is Southeast Asia, CA is Central Asia, and RA is Russia Asia.

Table 5. Asian emissions in 2006 and trends between 2006 and 2010 (units for emissions: Tg for CO$_2$ and Gg for other species)*.

Regions	SO$_2$	NO$_x$	CO	NMVOC	NH$_3$	PM$_{10}$	PM$_{2.5}$	BC	OC	CO$_2$
China	**34 597 (0.83)**	**23 719 (1.23)**	**179 626 (0.95)**	**20 715 (1.14)**	**11 203 (0.88)**	**19 342 (0.86)**	**13 752 (0.89)**	**1771 (1.00)**	**3486 (0.97)**	**7827 (1.29)**
Japan	838 (0.85)	2352 (0.81)	5888 (0.73)	1538 (0.77)	507 (0.94)	149 (0.76)	109 (0.74)	32 (0.63)	12 (0.68)	1241 (0.89)
Korea, DPR	233 (0.91)	293 (0.81)	5430 (0.83)	175 (0.79)	108 (1.02)	319 (0.83)	139 (0.83)	16 (0.86)	18 (0.94)	84 (0.85)
Korea, Republic of	446 (0.94)	1270 (0.84)	827 (1.01)	794 (1.07)	184 (1.03)	65 (1.91)	42 (2.04)	15 (1.55)	12 (0.69)	510 (1.06)
Mongolia	71 (1.39)	45 (1.37)	523 (1.4)	37 (1.29)	103 (0.93)	75 (1.46)	31 (1.49)	1 (1.58)	2 (1.72)	11 (1.38)
Other East Asia	**1588 (0.90)**	**3961 (0.83)**	**12 668 (0.82)**	**2544 (0.87)**	**903 (0.97)**	**607 (1.01)**	**321 (1.02)**	**65 (0.92)**	**44 (0.84)**	**1846 (0.94)**
India	**7476 (1.24)**	**7484 (1.28)**	**55 910 (1.21)**	**14 685 (1.15)**	**9015 (1.09)**	**5874 (1.21)**	**4327 (1.21)**	**887 (1.15)**	**2415 (1.05)**	**1892 (1.20)**
Afghanistan	2 (1.33)	111 (1.60)	279 (1.64)	96 (1.46)	131 (1.10)	14 (1.49)	13 (1.48)	5 (1.48)	7 (1.37)	2 (1.25)
Bangladesh	102 (1.30)	283 (1.30)	2332 (1.10)	711 (1.11)	889 (1.14)	283 (1.21)	203 (1.15)	30 (1.09)	113 (1.07)	67 (1.25)
Bhutan	4 (1.32)	11 (1.21)	256 (1.18)	43 (1.15)	42 (0.99)	21 (1.23)	18 (1.18)	3 (1.14)	12 (1.13)	4 (1.17)
Maldives	3 (0.97)	8 (0.98)	144 (1.05)	7 (1.21)	0 (1.07)	0 (1.28)	0 (1.27)	0 (1.45)	0 (0.40)	2 (1.00)
Nepal	28 (1.08)	72 (1.16)	1985 (1.06)	405 (1.09)	242 (1.05)	138 (1.08)	128 (1.08)	25 (1.08)	98 (1.08)	32 (1.07)
Pakistan	1128 (1.24)	816 (1.16)	8298 (1.12)	1871 (1.13)	1543 (1.20)	542 (1.11)	503 (1.11)	103 (1.11)	358 (1.09)	231 (1.14)
Sri Lanka	108 (1.23)	120 (0.96)	1274 (1.04)	347 (1.06)	112 (1.09)	123 (1.23)	98 (1.13)	15 (1.00)	58 (1.02)	29 (1.08)
Other South Asia	**1376 (1.24)**	**1421 (1.20)**	**14 568 (1.11)**	**3481 (1.12)**	**2959 (1.16)**	**1121 (1.15)**	**964 (1.12)**	**181 (1.10)**	**647 (1.08)**	**365 (1.15)**
Brunei	9 (1.22)	10 (1.15)	6 (0.91)	32 (0.98)	7 (1.13)	1 (0.56)	1 (0.58)	0 (0.67)	0 (0.53)	8 (1.18)
Cambodia	26 (0.99)	46 (1.00)	976 (1.05)	198 (1.07)	121 (1.11)	55 (1.06)	53 (1.06)	11 (1.04)	42 (1.04)	16 (1.04)
Indonesia	1676 (1.17)	1999 (1.29)	19 379 (1.23)	6134 (1.30)	1634 (1.19)	1237 (0.96)	944 (1.00)	164 (1.08)	663 (1.04)	520 (1.07)
Laos	133 (1.13)	35 (1.17)	388 (1.02)	80 (1.06)	78 (1.12)	24 (1.01)	22 (1.01)	4 (1.02)	16 (1.00)	6 (1.03)
Malaysia	290 (1.26)	505 (1.25)	3117 (1.20)	1504 (1.17)	222 (1.15)	191 (1.13)	126 (1.05)	14 (1.13)	33 (1.05)	175 (1.15)
Myanmar	71 (0.94)	76 (1.21)	2594 (1.04)	654 (1.25)	392 (1.08)	155 (1.06)	149 (1.04)	30 (1.04)	121 (1.03)	47 (1.05)
Philippines	474 (1.06)	288 (1.26)	2269 (1.03)	812 (1.07)	404 (1.02)	160 (1.21)	114 (1.08)	15 (0.97)	70 (0.98)	94 (1.27)
Singapore	191 (0.92)	112 (1.03)	138 (1.18)	290 (1.15)	12 (0.85)	7 (0.96)	6 (0.97)	1 (1.08)	1 (1.12)	39 (1.08)
Thailand	796 (0.77)	740 (1.09)	7555 (1.13)	2031 (1.15)	533 (1.22)	508 (0.97)	285 (0.96)	33 (1.06)	134 (1.11)	271 (1.09)
Vietnam	463 (1.24)	337 (1.31)	7419 (1.11)	1584 (1.41)	624 (1.07)	594 (1.20)	485 (1.16)	79 (1.09)	302 (1.06)	184 (1.26)
Southeast Asia	**4129 (1.08)**	**4149 (1.23)**	**43 841 (1.16)**	**13 319 (1.25)**	**4027 (1.14)**	**2933 (1.04)**	**2184 (1.04)**	**352 (1.07)**	**1383 (1.05)**	**1360 (1.12)**
Kazakhstan	1775 (0.59)	499 (1.12)	2107 (1.59)	423 (1.28)	39 (1.06)	381 (1.16)	192 (1.16)	10 (1.26)	191 (1.17)	191 (1.07)
Kyrgyzstan	30 (0.90)	27 (1.32)	224 (1.66)	30 (1.34)	12 (1.00)	60 (1.03)	27 (1.05)	1 (1.44)	2 (1.21)	5 (1.19)
Tajikistan	11 (1.24)	16 (1.62)	122 (1.57)	25 (1.17)	15 (1.06)	28 (0.80)	15 (0.86)	1 (1.78)	3 (1.34)	3 (1.03)
Turkmenistan	45 (1.42)	97 (1.28)	298 (1.40)	174 (1.37)	13 (1.10)	54 (1.18)	25 (1.20)	2 (1.37)	2 (1.28)	42 (1.22)
Uzbekistan	590 (0.84)	241 (0.94)	808 (1.11)	287 (1.08)	53 (0.94)	325 (1.15)	143 (1.15)	3 (1.03)	9 (1.13)	129 (0.94)
Central Asia	**2451 (0.67)**	**879 (1.10)**	**3558 (1.47)**	**940 (1.24)**	**131 (1.01)**	**847 (1.14)**	**402 (1.14)**	**17 (1.27)**	**39 (1.17)**	**370 (1.04)**
East Siberia	1711 (0.96)	482 (1.11)	2437 (1.18)	351 (1.12)	24 (0.97)	380 (0.97)	199 (0.99)	11 (1.28)	19 (1.06)	178 (1.03)
Far East	349 (1.02)	410 (1.19)	2284 (1.17)	268 (1.13)	20 (0.91)	228 (0.98)	120 (1.03)	17 (1.34)	22 (1.13)	109 (1.10)
Ural	1510 (0.98)	412 (1.11)	3757 (1.07)	551 (1.07)	22 (0.99)	1042 (1.01)	580 (1.03)	17 (1.09)	69 (1.09)	174 (1.07)
West Siberia	647 (1.05)	815 (1.14)	5399 (1.12)	1206 (1.09)	43 (0.99)	484 (0.96)	275 (0.98)	27 (1.19)	50 (1.03)	308 (1.10)
Russia Asia	**4217 (0.99)**	**2119 (1.13)**	**13 878 (1.12)**	**2376 (1.09)**	**108 (0.97)**	**2132 (0.99)**	**1173 (1.01)**	**72 (1.21)**	**160 (1.07)**	**770 (1.08)**
Asia	**55 832 (0.92)**	**43 732 (1.19)**	**324 049 (1.04)**	**58 059 (1.15)**	**28 348 (1.02)**	**32 857 (0.97)**	**23 124 (0.98)**	**3345 (1.06)**	**8174 (1.02)**	**14 430 (1.20)**

* numbers in the parentheses represent emission ratios of 2010 to 2006. Bold values are the total emissions and ratios for Asian regions.
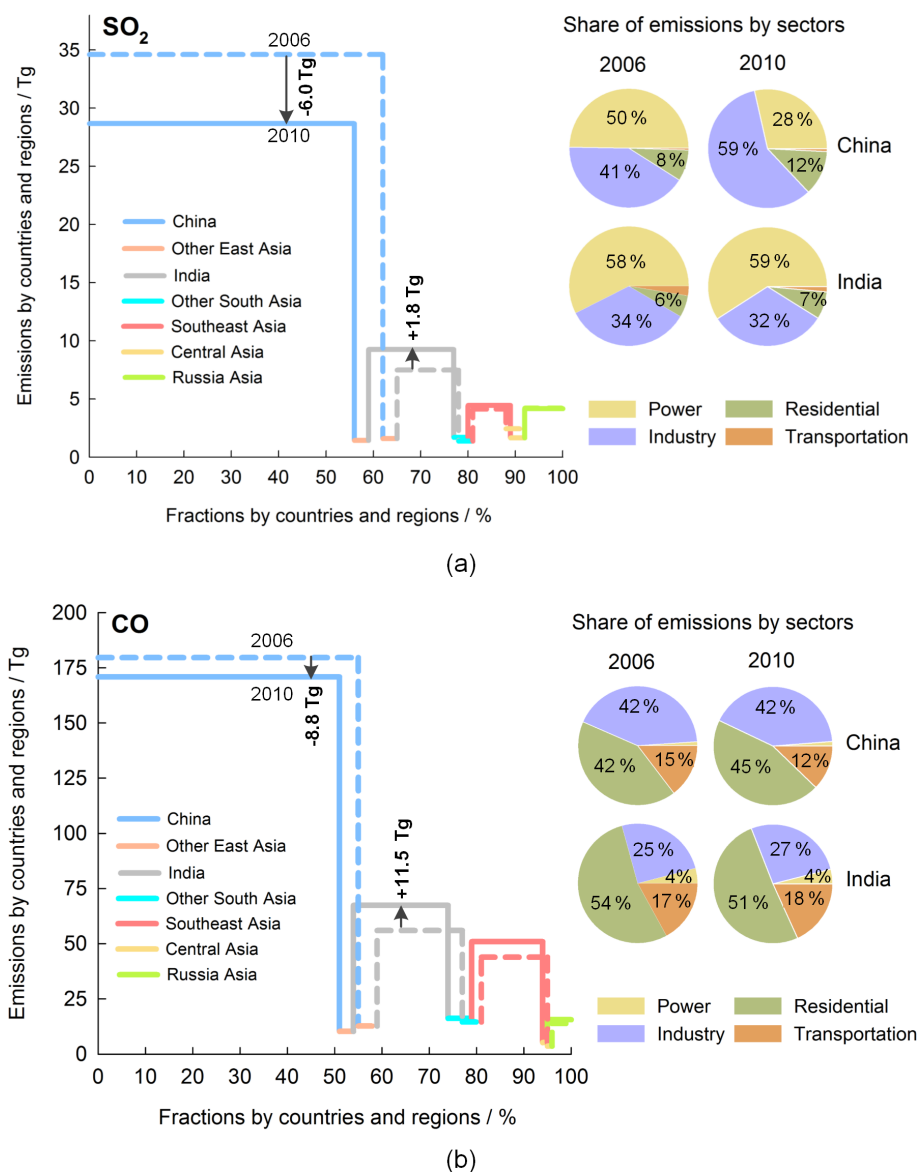
Figure 8. Emission changes from 2006 to 2010 by Asian regions for SO_2 **(a)** and CO **(b)**. Left panel: emissions in 2006 and 2010 by region. Y axis represents emissions by region. X axis represents accumulative emission contribution of regions. The dotted and solid lines represent emissions in 2006 and 2010 respectively. Right panel: the shares of emissions by sectors over China and India in 2006 and 2010.

total primary energy consumption of Asia has increased by 20.6 % during the period of 2005 and 2010 (IEA, 2013). During the same period, SO_2 emissions decreased in China (−17.2 %), Other East Asia (−9.5 %), and Central Asia (−32.8 %) due to effective emission control, while they increased in India (+23.9 %), Other South Asia (+23.9 %), and Southeast Asia (+7.8 %) due to growth in coal use and absence of desulfurization devices. The decrease in SO_2 emissions changes in Asian is dominated by changes in China and India. Figure 8a demonstrates the changes in SO_2 emissions among Asian regions from 2006 to 2010. Wide installation of FGD in China's coal-fired power plants is the main driving factor of SO_2 emission changes over Asia. SO_2

emissions in China's power plants decreased from 17.2 Tg in 2006 to 8.2 Tg in 2010, contributing to most of the total SO_2 emission reduction over Asia. In contrast, SO_2 emissions in India increased by 27 % during 2006–2010, owing to the dramatic construction of new power plants and the lack of emission control facilities (Garg et al., 2001, 2006). As a consequence, the Indian share of the total Asian SO_2 emissions increased from 13 % in 2006 to 18 % in 2010. NO_x and NMVOCs emissions were increased in all Asian regions except Other East Asia (−17.3 % for NO_x and −13.0 % for NMVOCs respectively), indicating lack of effective control measures for those two species over Asia. Increases of NO_x and NMVOC emissions are mainly driven by growth in in-

Table 6. Comparison of emission trends of NO_x, SO_2, and CO over Asia with satellite observations.

Species	Regions	Study	Method	Period	AGR (% yr^{-1})[a]
NO_x	China	Berezin et al. (2013)	Inverse modeling	2001–2008	11.5
	China	Gu et al. (2013)	Inverse modeling	2005–2010	4.0
	China	Miyazaki et al. (2016)	Inverse modeling	2005–2010	3.7
	East China	Mijling et al. (2013)	Inverse modeling	2007–2011	9.0
	East China	Krotkov et al. (2016)	Satellite	2005–2010	5.4
	Central East China	Itahashi et al. (2014)	Satellite	2000–2010	11.0
	China	This work	Inventory	2006–2010	5.2
	India	Krotkov et al. (2016)	Satellite	2005–2010	4.6
	India	Miyazaki et al. (2016)	Inverse modeling	2005–2010	3.2
	India	This work	Inventory	2006–2010	6.3
SO_2	East China	Krotkov et al. (2016)	Satellite	2005–2010	−6.9
	China	This work	Inventory	2006–2010	−4.6
	India	Krotkov et al. (2016)	Satellite	2005–2010	16.5
	India	This work	Inventory	2006–2010	5.5
CO	China	Yumimoto et al. (2014)	Inverse modeling	2005–2010	−3.1
	China	Yin et al. (2015)	Inverse modeling	2002–2011	−1.1
	East China	Worden et al. (2013)	Satellite	2000–2012	−1.6, −1.0[b]
	China	This work	Inventory	2006-2010	−1.2

[a] AGR is annual growth rate. [b] Results are developed using MOPITT and AIRS.

dustrial activities and vehicle population. For NO_x, remarkable emission increases are observed for China (+22.6 %), India (+27.8 %), Other South Asia (+20.5 %), and Southeast Asia (+23.4 %) during 2006–2010. For NMVOC, emissions increased by 14.0, 15.0, 12.3, 24.9, 23.6, and 9.3 % for China, India, Other South Asia, Southeast Asia, Central Asia, and Russia Asia respectively. Emission changes of other species are relatively small (i.e., within 6 %) during 2006–2010. For CO, PM_{10}, and $PM_{2.5}$, emission reductions in China were partly offset by increases of emissions in the South and Southeast Asian regions. CO emissions in China decreased by 5 % during 2006–2010 (see Fig. 8b), mainly due to improved combustion efficiency, recycling of industrial coal gases, and strengthened vehicle emission standards. The implementation of new vehicle emission standards and retirement of old vehicles has reduced China's transportation CO and NMVOC emissions by 20 and 30 %, respectively, during 2006–2010. While in India, Other South Asia, and Southeast Asia, CO emissions increased by 21, 11, and 16 %, respectively, between 2006 and 2010.

Satellite observations have shown promising capabilities in detect trends in surface emissions (Streets et al., 2013). The increases in NO_x emissions over China and India were confirmed by satellite-based inversions and the growth rates in satellite-based NO_x emission trends during 2006–2010 are generally comparable to our estimates in emission inventories (Table 6). For SO_2 emissions, the downward trend over China and upward trend over India were also observed by satellite remote sensing, while higher growth rates were detected by OMI than the bottom-up emission inventory

(Krotkov et al., 2016). The downward trend of CO emissions over China in recent years has been confirmed by both in situ and satellite observations (Wang et al., 2010; Worden et al., 2013; Yumimoto et al., 2014; Yin et al., 2015). The decreasing rate of CO emissions over China is estimated to be -1.2 % yr^{-1} from 2006 to 2010 in the MIX inventory, consistent with the rates observed by multiple satellites in range of -1.0 to -3.1 % yr^{-1} during 2000–2012 (Table 6).

3.3 Speciated NMVOC emissions

Figure 9 presents 2010 Asian NMVOC emissions of different chemical groups by region and by sector. Similar to Asian emissions estimated in previous work (Klimont et al., 2002; Li et al., 2014), alkanes and alkenes are the largest contributors to the total Asian NMVOC emissions in 2010 (27 and 26 % of the total respectively), followed by oxygenated volatile organic compounds (OVOCs; 20 %), aromatics (17 %), and alkynes (7 %). Regionally, shares of alkanes and aromatics are higher in China, Other East Asia, Central Asia, and Russia Asia than other regions, due to large contributions from the industrial sector. Shares of alkynes in Central Asia and Russia Asia are significantly lower than other regions due to a low contribution from biofuel emissions. Sectoral contribution of emissions varies significantly by different chemical groups. Over Asia, the industrial sector is the major source of emissions of alkanes and aromatics. Alkanes emissions from industrial sector are mainly contributed by gas production and distribution (19.8 % of total industrial emissions), coal combustion (17.1 %), and oil
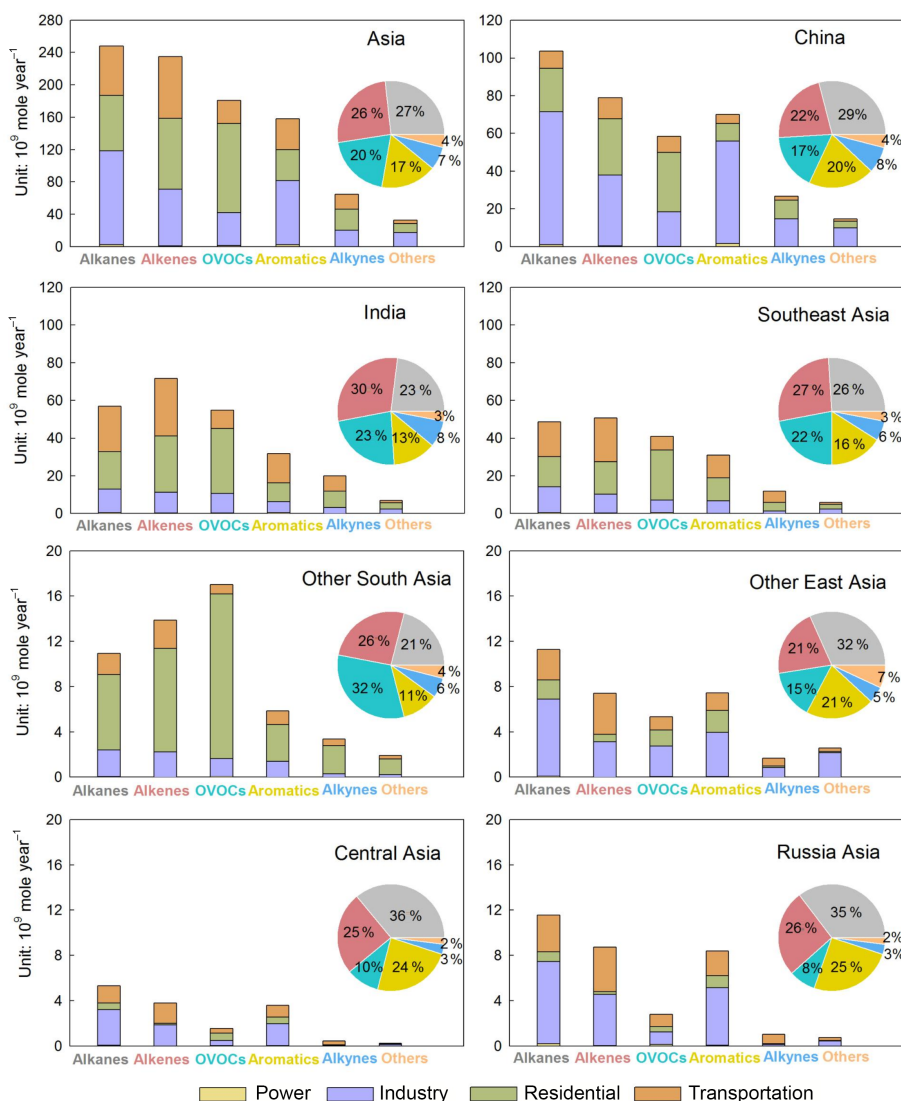
Figure 9. Speciated NMVOC emissions for the year 2010 by chemical group and by Asian regions. Alkanes: ethane, propane, butanes, pentanes, hexanes, higher alkanes and their isomers. Alkenes: ethane, propene, isoprene, terpenes, higher alkenes and their isomers. Alkynes: ethyne and other alkynes. Aromatics: benzene, toluene, xylene, trimethylbenzene, other aromatics and their isomers. OVOCs: aldehydes (formaldehyde, acetaldehyde, and higher aldehydes), ketones (acetone and higher ketones), alcohols (methanol, ethanol, and higher alcohols), ethers, and acids. "Others": halogenated hydrocarbons, unidentified species, etc.

refinery (15.0 %), and aromatics emissions are mainly contributed by architectural paint use (21.0 % of total industrial emissions), other industrial paint use (16.6 %), and gas production and distribution (10.6 %). The residential sector has a high contribution of OVOCs, alkynes, and alkenes, among which mainly contributed by biofuel combustions. The sectoral contribution to different chemical groups also varies with region. For example, the residential sector dominates emissions for all species in the Other South Asia region, as a consequence of the low economic development in that region.

Among different regions, China, India, and Southeast Asia are the largest contributors to NMVOC emissions in Asia,

with contributions varying by chemical groups. China contributes more than 40 % of alkanes, alkynes, and aromatics in Asia, compared to 35 % contribution of the total Asian NMVOC emissions. India contributes high to emissions of alkenes, alkynes, and OVOCs, constituting about 30 % of Asian emissions. The high emissions of alkenes in India (and Other South Asia) are mainly from contributions of biofuel combustions and motorcycles, and OVOC emissions in India are dominant by biofuel combustions. Southeast Asia shares around 20 % of the emissions of alkanes, alkenes, aromatics, and OVOCs.
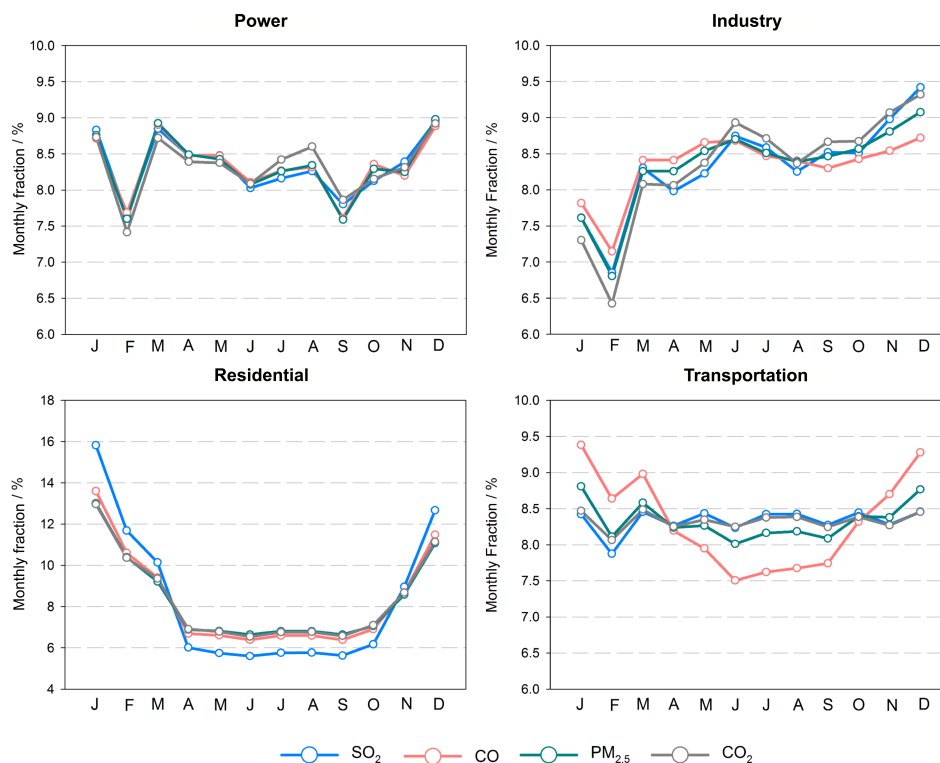
Figure 10. Monthly variations of Asian SO_2, CO, $PM_{2.5}$, and CO_2 emissions by sector for the year 2010.

3.4 Seasonality

Monthly emissions by sector and by Asian region are provided in Tables S6–S14. Monthly profiles in emissions are highly sector dependent given that monthly activity rates vary among different sectors. Figure 10 illustrates the monthly variations of Asian SO_2, CO, $PM_{2.5}$, and CO_2 emissions by sector for the year 2010. Different species generally show similar monthly emission patterns within the same sector, indicating that monthly emission profiles of each sector are dominated by monthly variations in activity rates. For example, industrial emissions are higher in the second half of the year induced by larger industrial productions to meet the annual total production target. The most significant monthly variation with a winter peak was found in the residential sector, reflecting the higher energy demand for residential heating in winter. Residential SO_2 emissions in winter are even higher than other species, because SO_2 emissions from China dominate residential emissions in Asia (70 % of total), of which coal consumption in winter is higher than other regions for heating. Monthly profiles of CO emissions are different from other species for the transportation sector. This is because the CO emission factor in winter is higher than in other seasons due to additional emissions from the cold-start process (Kurokawa et al., 2013; Zheng et al., 2014).

Figure 11 presents monthly variations of SO_2, CO, $PM_{2.5}$, and CO_2 emissions by Asian region. Compared to other species, CO emissions are much higher in winter in high-latitude regions due to residential heating and additional vehicle emissions from cold starts. Winter $PM_{2.5}$ emissions in China are higher than other regions, representing large emissions from solid fuel use in residential homes.

3.5 Gridded emissions

In the MIX inventory, gridded emissions for 10 gaseous and aerosol species were developed at $0.25 \times 0.25°$ resolution. Emission maps of all species in 2010 are shown in Fig. 12. Compared to the previous gridded Asian emission inventories, we believe the spatial patterns are improved because several local high-resolution emission datasets are incorporated, such as CPED for China and JEI-DB and OPRF for Japan. However, for sectors in which emissions are dominated by spatially scattered sources (e.g., residential combustion, solvent use), the spatial distributions in emissions are still uncertain.

MIX emission inventory can be accessed publicly from the website of http://www.meicmodel.org/dataset-mix. Both 2008 and 2010 emissions of 10 species with monthly variation at a spatial resolution of $0.25 \times 0.25°$ are available from the website, including SO_2, NO_x, CO, NH_3, NMVOC, PM_{10}, $PM_{2.5}$, BC, OC, and CO_2. Speciated NMVOC Emissions for CB05 and SAPRC-99 chemical mechanisms are provided at the same spatial and temporal resolution. The MIX in-
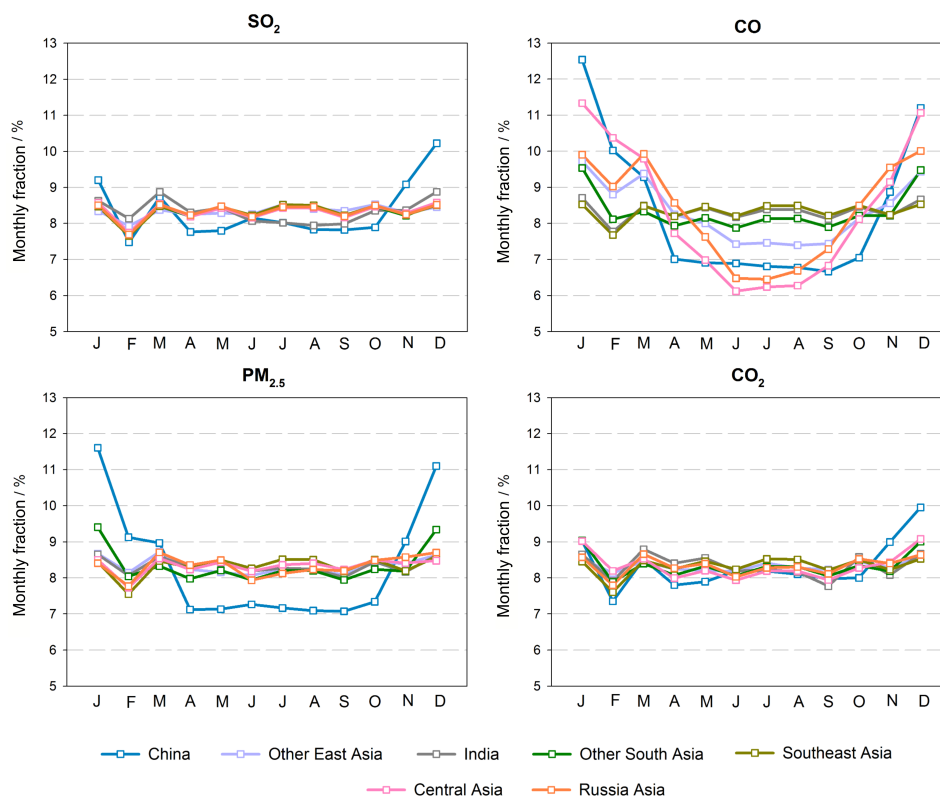
Figure 11. Monthly variations of SO_2, CO, $PM_{2.5}$, and CO_2 emissions by Asian region for the year 2010.

Table 7. Intercomparisons of total anthropogenic emissions[a] among MIX, REAS2, and EDGAR v4.2 for 2008.

Unit: Tg yr^{-1}	SO_2	NO_x	CO	NMVOC	NH_3	PM_{10}	$PM_{2.5}$	BC	OC	CO_2
				Asia[b]						
MIX	49.00	46.38	317.11	60.26	27.66	30.16	21.71	3.40	8.04	15 145
REAS2	52.82	46.17	344.20	65.94	32.74	34.21	23.51	2.95	7.55	15 271
EDGAR v4.2	63.26	36.73	212.16	53.43	20.08	31.08				15 282
				China						
MIX	31.41	26.55	175.64	22.10	9.80	17.63	12.74	1.76	3.38	8955
REAS2	33.58	25.55	202.71	27.78	15.00	21.69	14.57	1.60	3.09	9085
EDGAR v4.2	41.35	20.66	106.10	22.60	11.11	14.76				8647
				India						
MIX	8.42	8.86	61.80	15.95	9.42	6.65	4.88	0.98	2.48	2103
REAS2	10.08	9.68	61.80	15.95	9.42	6.65	4.88	0.71	2.29	2103
EDGAR v4.2	8.42	6.37	45.58	10.58	4.14	10.80				2307

[a] Including power, industry, residential, transportation, and agriculture. [b] "Asia" refers to all Asian regions excluding the Russia Asia in MIX.

ventory has been regridded to $0.1 \times 0.1°$ resolution using the area-weighting approach and then incorporated to the HTAP v2 gridded emission inventory (Janssens-Maenhout et al., 2015). The HTAP v2 emission inventory can be downloaded from the EDGAR website (http://edgar.jrc.ec.europa.eu/htap_v2/index.php?SECURE=_123).

4 Comparison with other inventories

4.1 MIX, REAS2, and EDGAR v4.2 over Asia

A comprehensive intercomparison among different emission inventories over Asia was conducted by Kurokawa et al. (2013). In this work, we compare the MIX inventory
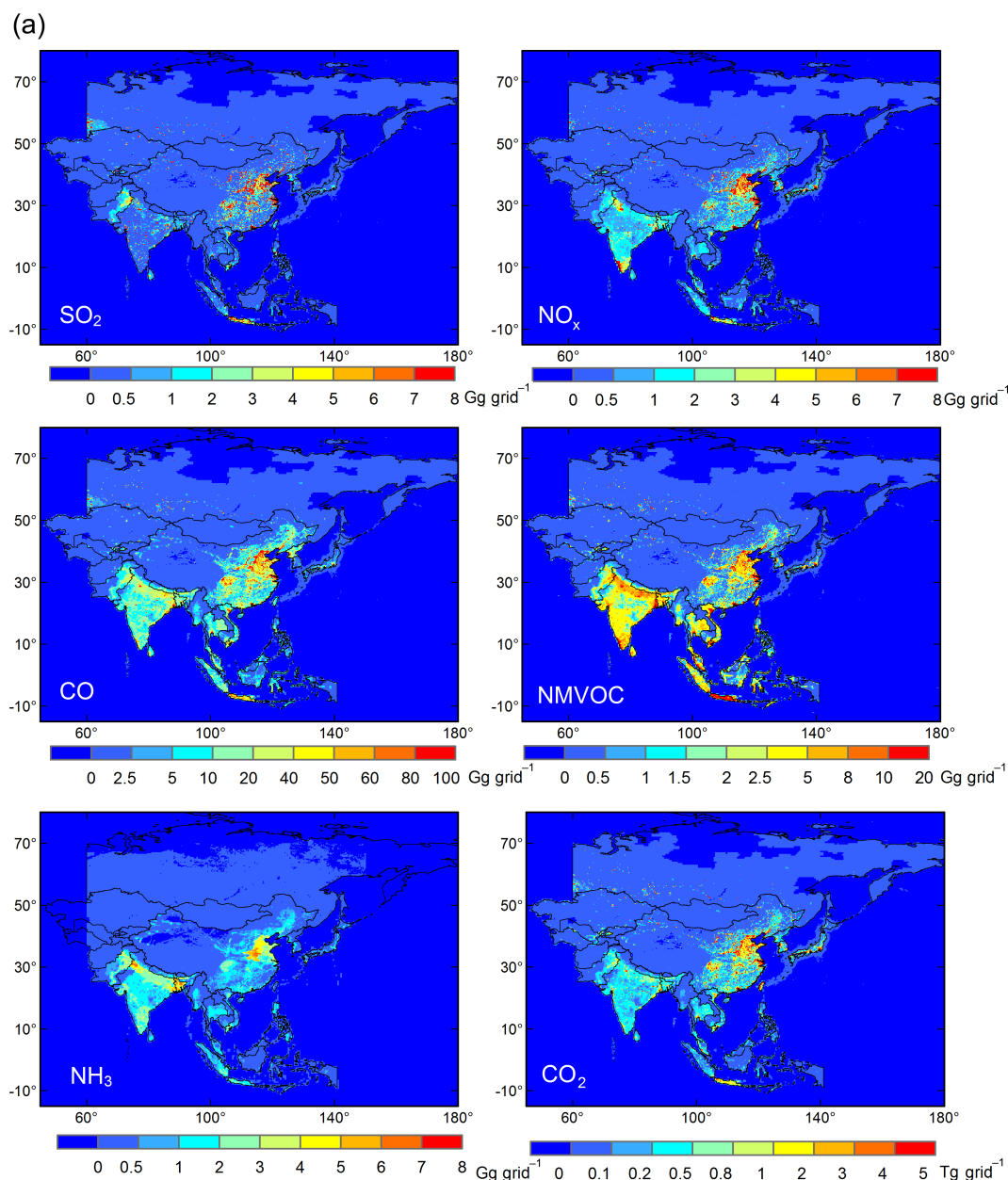
Figure 12.

with REAS2 and EDGAR v4.2 (EC-JRC/PBL, 2011), two widely used inventories, to highlight the new findings from the mosaic inventory and identify the potential sources of uncertainties. We choose the year of 2008 to conduct the comparison because emissions after 2008 are not available in either REAS2 or EDGAR v4.2. Russian Asia was excluded from comparison. Asian anthropogenic emissions of MIX, REAS2, and EDGAR v4.2 in 2008 are tabulated in Table 7. Over Asia, MIX and REAS differ within 10 % for most species, except for NH_3 (18 % higher in REAS), PM_{10} (13 % higher), and BC (13 % lower). It is not surprising that the total Asian emission budgets in MIX and REAS2 are simi-

lar given that MIX used emissions estimates in REAS2 for Asian regions except China and India. However, REAS2 has incorporated several recent emission inventories for China (Kurokawa et al., 2013). The differences between REAS and MIX over China and India will be discussed in the following sections.

Remarkable differences are observed between MIX and EDGAR v4.2. Compared to MIX, 2008 Asian emissions in EDGAR are 29 % higher for SO_2, but 20, 33, 11, and 27 % lower for NO_x, CO, NMVOC, and NH_3 respectively. PM_{10} and CO_2 emissions agree well between the two inventories with differences within 3.2 %. Figure 13 details the differ-
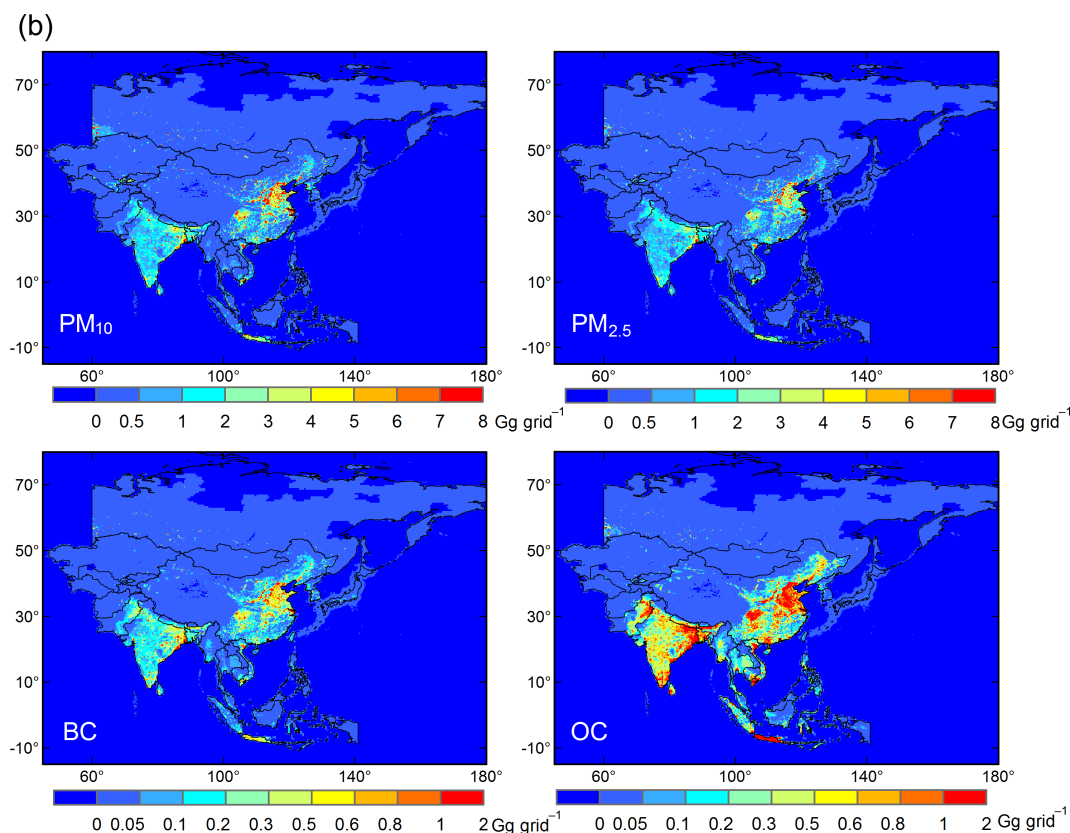
Figure 12. Grid maps for gaseous **(a)** and aerosol **(b)** species in the MIX Asian emission inventory, 2010.

ences by region and by sector. Regionally, the differences can be largely attributed to disagreements in emission estimates for China and India, as presented in Table 7. Discrepancies are relatively large at the sector level compared to total emissions. EDGAR's estimates for SO_2 emissions from power plants are 60 % higher than estimates in MIX. For China, 70 % of power generation capacities were equipped with FGD and the average SO_2 removal efficiency was 78 % (Liu et al., 2015). The high estimates in EDGAR v4.2 are most likely due to underestimation of FGD penetration or SO_2 removal efficiencies of FGD (Kurokawa et al., 2013). Remarkable differences for the residential and transportation sectors are found for NO_x, CO, and NMVOC estimates in the two inventories. For instance, EDGAR v4.2 estimates lower NO_x emissions of transportation sector by 27 and by 48 % for the residential sector compared to MIX. Similarly, residential CO emissions in EDGAR v4.2 are 33 % lower than in MIX, leading to 33 % lower estimates of CO emissions in EDGAR v4.2 compared to MIX. Underestimates of CO emissions in EDGAR v4.2 inventory have been confirmed by top-down constraints (Pétron et al., 2004; Fortems-Cheiney et al., 2011). As the statistical differences of energy use are usually within 30 % at sector level (Guan et al., 2012), the discrepancy by sector could only be attributed to differences in the raw emission factors and abatement measures. Al-

though a point-by-point comparison of emission factors between EDGAR v4.2 and MIX is not feasible, we can still speculate that EDGAR v4.2 may overestimate the combustion efficiency and emission control measures in Asia by using an emission factor database from developed countries. NH_3 emissions in EDGAR v4.2 are 26 % lower than in MIX, with a large difference in residential emissions. The differences are mainly from high emission estimates of wastewater treatment sources in REAS2, which were incorporated into MIX for Asian regions except China. MIX estimated 3.4 Tg NH_3 emissions from wastewater treatment in Asia in 2008, which are more than 2 orders of magnitude higher than EDGAR v4.2 estimates. Differences in PM_{10} emissions at the sector level are also large; similar estimates of PM_{10} emissions in the two datasets are rather a coincidence than real agreements.

For CO_2 emissions, good agreements are found among MIX, REAS2, and EDGAR v4.2 inventories in Asia with differences in total emissions less than 1 %. CO_2 emissions from biofuel combustion are included in the intercomparison. CO_2 emission estimates in MIX and REAS2 only differ in China because REAS2 are used in MIX for regions other than China. Total CO_2 emissions of China in MIX and REAS2 are quite similar (1.5 % higher in REAS2), while REAS2 estimated higher emissions for power sector (+386 Tg or
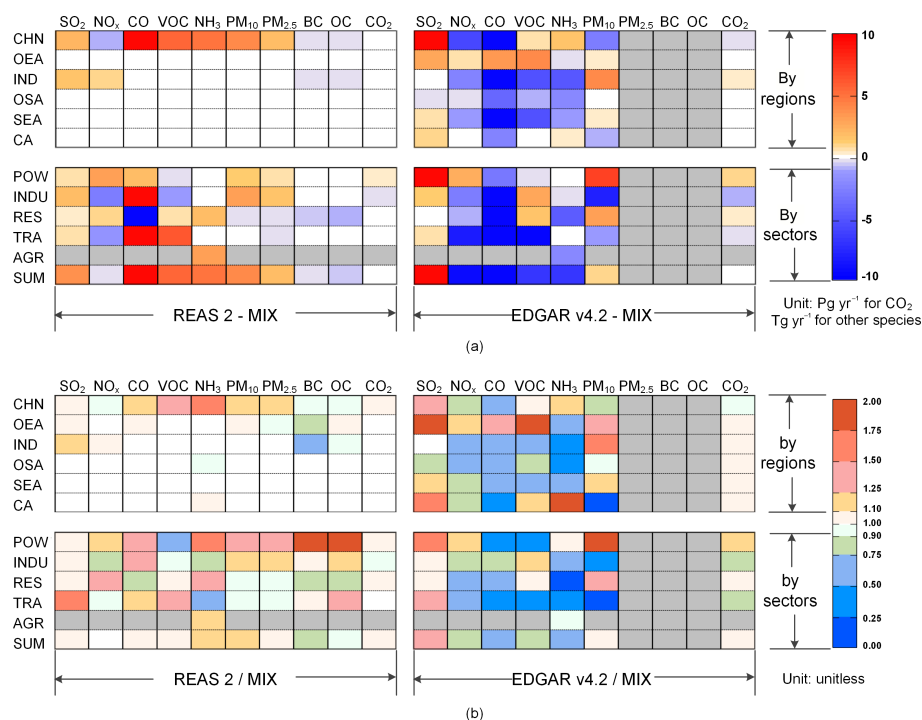
Figure 13. Intercomparisons of emission estimates between MIX, REAS2, and EDGAR v4.2 by Asian regions and sectors. **(a)** Absolute differences of emission estimates. **(b)** Ratio of emission estimates. Grey shaded grids indicate that the comparison is not available due to absence of emission estimates in EDGAR v4.2. Abbreviations of Asian countries and regions are the same as in Fig. 7. Abbreviations of sectors are as follows: POW is power plants; INDU is industry; RES is residential; TRA is transportation; AGR is agriculture; SUM is total. Russia Asia is not included in the comparison.

+13.6 % compared to MIX) but lower emissions for industry (−293 Tg, −6.8 %) emissions. EDGAR v4.2 estimates lower CO_2 emissions for China (−308 Tg, −3.4 %) and higher emissions for other regions: +102 Tg (+5.6 %) for Other East Asia, +83.9 Tg (+5.6 %) for Southeast Asia, +204 Tg (+9.7 %) for India, +29.5 Tg (+7.5 %) for Other South Asia, and +25.3 Tg (+6.4 %) for Central Asia. At sector level, EDGAR v4.2 estimates are 29 % (+833 Tg) higher for power, 22 % (−944 Tg) lower for industry, and 31 % (−192 Tg) lower for transportation over China compared to MIX. For Other East Asia, differences between EDGAR v4.2 and MIX are mainly contributed by power sector, with 20 % higher emissions (+130 Tg) in EDGAR v4.2. Residential sector is the main contributor to the differences between EDGAR v4.2 and MIX over India, with 28 % (+177 Tg) higher emissions estimated in EDGAR v4.2. The relatively large discrepancy at sector level can be attributed to differences in energy statistics and emission factors (Guan et al., 2012; Liu et al., 2015) as well as differences in sector definitions. In particularly, EDGAR v4.2 used fuel consumption data from IEA statistics while MIX and REAS2 used provincial level data from Chinese Energy Statistics, which can differ by 20 % at sector level (Hong et al., 2016). Emissions from heating plants are aggregated to the industrial sector in the MIX inventory, while in EDGAR v4.2 heating plants

are aggregated to the energy sector and then compared to the power sector in the MIX inventory. In the future, harmonizing the sector (subsector) definition among global and regional inventories would help to reduce the discrepancy of emission estimates at sector level.

4.2 China

4.2.1 Power plants

Both MIX and REAS2 processed power plants emissions as point sources. As presented in Sect. 2.2, MIX used a high-resolution emission database for China (CPED; Liu et al., 2015) to derive emissions and locations of China's power plant emissions at unit level. In REAS2, emissions of individual power plants are estimated by combining information from two global databases, CARMA and WEPP. MIX and REAS2 showed good agreements on power plant emissions in China for SO_2 and CO_2 (8 % differences for SO_2 and 14 % for CO_2) in 2008, implying similar estimates in energy consumption and emission factors in two inventories. Compared to MIX, REAS2 estimates higher emissions of NO_x, PM_{10}, and $PM_{2.5}$ by more than 20 %, mainly due to the differences in the emission factors used in compiling China's emissions. Liu et al. (2015) found that CARMA has omitted information of small plants and overestimated emissions
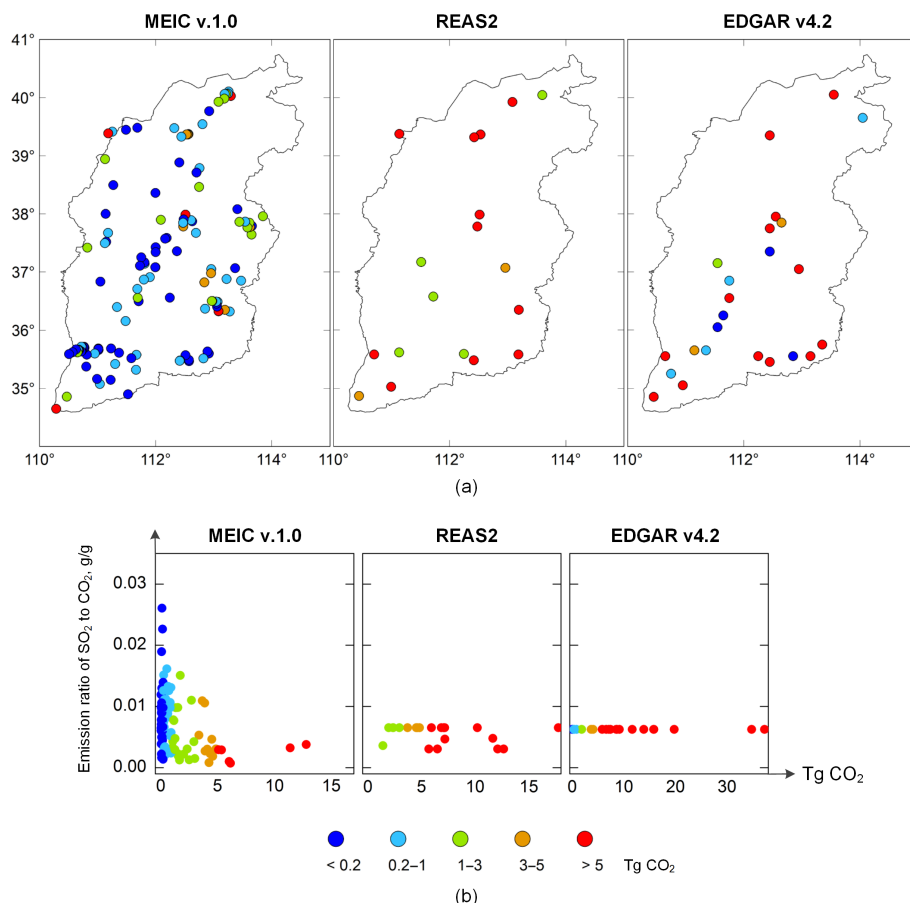
Figure 14. Comparison of 2008 power plants emission estimates between MEIC v1.0, REAS2, and EDGAR v4.2 for Shanxi province, China. **(a)** Spatial distribution of CO_2 emissions and **(b)** emission ratios of SO_2 to CO_2. CO_2 emissions are grouped by colors.

from large plants by wrongly allocating fuel consumptions of small plants to large ones. REAS2 included 380 power plants for China, compared to 2411 plants in MIX, while power plants in REAS2 are large ones which contributed 72 % of CO_2 emissions in China.

Figure 14a compares CO_2 emissions from power plants between MEIC and REAS2 in Shanxi province where a large amount of coal is extracted and combusted in power plants. EDGAR emissions are also presented in Fig. 14a as a reference. For Shanxi province, MIX, REAS2, and EDGAR included 134, 22, and 24 coal-fired power plants, respectively, demonstrating the omission of many small power plants in REAS2 and EDGAR. In REAS2, only plants with annual CO_2 emissions higher than 1 Tg were processed as point sources (Kurokawa et al., 2013). In the three datasets, a total of 6, 13, and 12 power plants in Shanxi province have annual CO_2 emissions higher than 5 Tg, respectively, indicating significant emission overestimates for large plants in REAS2 and EDGAR. Moreover, the locations of power plants are not accurate in EDGAR given that CARMA used city centers as the approximate coordinates of power plants (Wheeler and Ummel, 2008). In contrast, coordinates in CPED are

obtained from official sources and crosschecked by Google Earth (Liu et al., 2015); the positions of large power plants in REAS2 are also checked manually (Kurokawa et al., 2013).

Figure 14b further compares the emission ratios of SO_2 / CO_2 in the three inventories for individual power plants over Shanxi. Large deviations of SO_2 / CO_2 ratios in MIX are driven by variations of fuel quality, combustion efficiency, and FGD removal efficiency in each plant, which are precisely represented in CPED. In CPED, there is a tendency towards a decrease in SO_2 / CO_2 emission ratio with increase of plant size (corresponding to higher CO_2 emissions), in accordance with the legislation that large units were required to be equipped with FGD during 2005–2010 (Zhang et al., 2012). Smaller deviations in SO_2 / CO_2 emission ratios are found in REAS2, because power plant SO_2 emissions in REAS2 were estimated by using the average FGD penetration rates at provincial level (Kurokawa et al., 2013). The constant ratios for all power plants in EDGAR indicate that (a) the emission factors are not varied within China and (b) the spatial distribution treats all power plants equal, which does not take the variations among power plants into consideration.
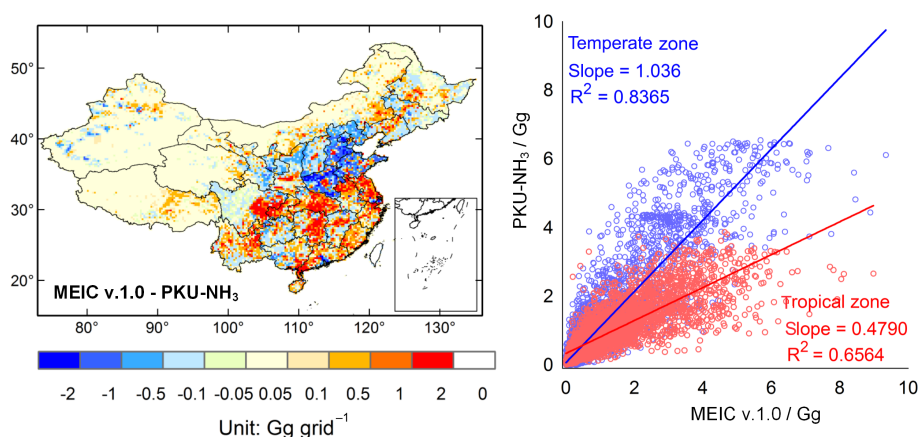
Figure 15. Comparisons of spatial distribution of NH_3 agricultural emissions between MEIC v1.0 and PKU-NH_3. Provinces that included in tropical zones are Fujian, Guangdong, Hainan, Guangxi, Guizhou, Hubei, Hunan, Yunnan, Sichuan, Jiangxi, Anhui, Zhejiang, and Jiangsu. Other provinces are treated as temperate ones.

Table 8. NH_3 agriculture emission estimates for China.

Unit: Tg-NH_3 yr^{-1}	PKU-NH_3	MEIC v1.0	REAS2	EDGAR v4.2	MASAGE_NH_3
Year	2006	2008	2008	2008	2005–2008*
Fertilizer application	3.20	4.40	9.40	8.26	3.64
Live stock	5.30	5.30	2.80	2.31	5.83

* Averaged estimates during 2005–2008.

4.2.2 Agriculture

The agriculture sector is a dominant source of NH_3 emissions, mainly contributed by fertilizer applications and manure managements. MIX incorporated the PKU-NH_3 inventory for China, which estimated agricultural NH_3 emissions using a process-based model to represent the dynamic impact of fertilizer use patterns, meteorological factors, and soil properties (Huang et al., 2012). The new inventory improved on previous studies which used uniform emission factors across time and region. Table 8 compares agricultural NH_3 emissions in China estimated in different emission inventories. Compared to other work, PKU-NH_3 yields lower estimates for fertilizer application but higher estimates for manure management. The differences are mainly because PKU-NH_3 used local correction factors for fertilizer volatilization and manure loss rate (Huang et al., 2012). Top-down inversion of NH_3 emissions by adjoint model and deposition fluxes agrees well with Huang et al. (2012), confirming the validity of the process-based model (Paulot et al., 2014).

Besides the magnitude of emissions, a process-based model may also better represent the spatial and temporal variations in emissions. As an example, Fig. 15 compares NH_3 agricultural emissions for MEIC and the PKU-NH_3 inventory for different climate zones. MEIC agrees well with PKU-NH_3 in temperate zones but is significantly higher than PKH-NH_3 in tropical zones. The differences in spatial dis-

tributions can be explained by the discrepancies in derived emission factors in the two inventories given that they used the same activity data from the National Bureau of Statistics of China (NBSC). MEIC used a higher loss rate of NH_3 (20 % for urea) for tropical zones and a lower one (15 %) for temperate zones following Klimont (2001). With full consideration of fertilization method and soil acidity by grids and by month, PKU-NH_3 estimated 9 % average NH_3 loss rate for urea for tropical zones and 14 % for temperate zone.

4.2.3 Other sectors

This section further discusses the differences between MIX and REAS2 over China. EDGAR is not compared here because references to the detailed underlying data used in EDGAR are not available. Figure S1 in the Supplement compares MIX and REAS2 estimates for China for 2008 by species and by sector. The two inventories generally agree well given that both MEIC and REAS2 incorporate the most recent advances in emission inventory studies in China. The major differences between the two inventories are discussed below with explanation for possible reasons.

REAS2 estimates higher CO and PM emissions than MEIC for the industrial sector. This is probably because REAS2 underestimates the emission control progress in China's industrial sector after 2005. During the 11th Five-Year Plan (2005–2010), China has implemented a series of

new standards to restrict industrial emissions, leading to a downward trend in emission factors after 2005 (Zhao et al., 2013). Emission standards implemented during 2005–2010 are summarized in Table S15. For the industrial sector, REAS2 adopted CO and PM emission factors from Streets et al. (2006) and Lei et al. (2011), respectively, which represent the real-world emission characteristics before the year 2005. Using those emission factors may have overestimated industrial emissions. Moreover, REAS2 estimated an increasing trend in China's CO emissions during 2005–2008, which is opposite to the downward trend derived from satellite-based constraints for the same period (Yumimoto et al., 2014; Yin et al., 2015), confirming that REAS2 may overestimate CO emissions in China after 2005. Transportation emissions in MEIC and REAS2 differ significantly for different species. Compared to REAS2, MEIC estimates much lower emissions for CO and NMVOC (dominated by gasoline vehicles) but higher emissions for NO_x and PM (dominated by diesel vehicles).

4.3 India

For India, MIX used ANL-India for SO_2, BC, and OC emissions and REAS2 for other species. Here we compare ANL-India and REAS2 for SO_2, BC, and OC emissions, to evaluate the impact of using ANL-India. Both ANL-India and REAS2 used energy consumption data from IEA, and hence the differences are mainly from emission factors. Reasonable agreements are found in total emissions over India (differing by 8–28 %), while discrepancies are large at the sector level. REAS2 estimates 50 % higher SO_2 estimates for all sectors except power plants, most likely from different assumptions about the sulfur content of fuels. For BC and OC, the ratio between REAS2 and ANL-India varies from 0.4 to 11.8 at the sector level, indicating large differences in emission factor selections. ANL-India used emission factors from a global database (Bond et al., 2004) with updates of a few recent measurements (Lu et al., 2011), while REAS2 used a local database developed many years ago (Reddy and Venkataraman, 2002a, b). It should be noted that local emission measurements in India are still too few to support accurate emission estimates. More measurements should be conducted in the future to remedy this situation.

When implementing REAS2 to MIX over India, power plant emissions were redistributed using spatial distributions derived from ANL-India at $0.25° \times 0.25°$ resolution (see Sect. 2.3). We believe that it will improve the accuracy because power plant emissions in ANL-India were estimated by each unit and allocated manually by Google Earth. A total of 68 power plants are identified in REAS2, compared to 145 plants in ANL-India. The two inventories generally agree well for the grids in which both inventories allocate power plant emissions. Lu and Streets (2012) found that the magnitudes and locations of power plant NO_x emissions (from ANL-India) are matched well with satellite-based ob-

servations over India, providing confidence to the accuracy of ANL-India estimates. From all the comparisons discussed above, we can conclude that emissions are well depicted in MIX due to integration of the most recent regional inventories.

5 Uncertainties and limitations

The MIX emission inventory subjects to uncertainties and several limitations. Emission estimates from bottom-up inventories are uncertain due to lack of complete knowledge of human activities and emission from different sources. Uncertainty ranges of an emission inventory could be estimated using propagation of error or Monte Carlo approaches (e.g., Streets et al., 2003; Zhao et al., 2011). However, in a mosaic emission inventory like MIX, a normalized quantitative assessment of uncertainty ranges is difficult because detailed information for emission inventory development is not collected. Table 9 summarized the uncertainty range estimates for China, India, and other Asian regions in different regional emission inventories. It should be noted that those ranges are not directly comparable due to differences in methods (propagation of error or Monte Carlo simulation). However, those numbers might roughly represent the uncertainty ranges in the MIX inventory as it was compiled from several inventories listed in Table 9. In general, uncertainty ranges are relatively small for species which emissions are dominated my large-scale combustion sources (e.g., SO_2, NO_x, and CO_2) but larger for species whose emissions are mainly from small-scale and scattered sources (e.g., CO, NMVOC, and carbonaceous aerosols). More detailed discussions on the uncertainty sources of Asian emission inventories can be found in previous literatures (e.g., Lu et al., 2011; Zhao et al., 2011; Kurokawa et al., 2013).

As indicated by Janssens-Maenhout et al. (2015), the mosaic process could introduce additional and undesired uncertainties when compiling a gridded emission inventory from different datasets. The uncertainties may arise from inconsistencies among datasets, including missing species in specific datasets, closure of mass balances for aerosols, and inconsistency on the country boarders.

When species in a specific inventory were missing, alternative estimates or datasets were used to fill the gap in which may involve additional uncertainties. In the MIX inventory, $PM_{2.5}$, BC, and OC emissions for Republic of Korea were roughly estimates from PM_{10} emissions in the CAPSS inventory and sector-specific emission ratios between PM_{10} and other aerosol components from Lei et al. (2011). For India, we used ANL-India for SO_2, BC, and OC for all sectors and NO_x for power plants. REAS2 was used to fill the gap where emissions from ANL-India were absent (see Sect. 2.3 for detailed process procedure). For above cases where estimates of different species in the same country were obtained from

Table 9. Uncertainty in emission estimates by Asian regions in 2010 (95 % confidence intervals; unit: %).

Regions	SO$_2$	NO$_x$	CO	NMVOC	NH$_3$	PM$_{10}$	PM$_{2.5}$	BC	OC	CO$_2$	References
China	±12	±31	±70	±68		±132	±130	±208	±258		Zhang et al. (2009)
						±91	±107	±187	±229		Lei et al. (2011)
	−14–13	−13–37				−14–45	−17–54	−25–136	−40–121		Zhao et al. (2011)
	−16–17							−43–93	−43–80		Lu et al. (2011)
	±31	±37	±86	±78	±153	±114	±133	±176	±271	±31	Kurokawa et al. (2013)
India	−15–16							−41–87	−44–92		Lu et al. (2011)
	±32	±49	±114	±137	±144	±120	±145	±178	±233	±49	Kurokawa et al. (2013)
Others	±35	±47	±131	±111	±148	±194	±208	±257	±286	±44	Kurokawa et al. (2013)

various sources, the ratios between species may be less reliable and should be used with caution.

When using different datasets for different types of aerosols in the same country, additional uncertainties for aerosol emissions might be introduced from the inconsistency in mass balance closure due to differences in spatial proxies (Janssens-Maenhout et al., 2015), which is the case for Indian emissions in this study. In the MIX inventory, BC and OC emissions were obtained from ANL-India while PM$_{2.5}$ and PM$_{10}$ emissions were taken from REAS2. During the mosaic process of Indian emissions, an additional check was performed by grid for each sector and emissions of PM$_{2.5}$ were adjusted to the sum of BC and OC emissions for the grids where the sum of BC and OC emissions exceeds PM$_{2.5}$ emissions.

For a mosaic emission inventory, inconsistencies could occur at country boarders when emissions of the two adjacent countries were obtained from different datasets (Janssens-Maenhout et al., 2015). In the MIX inventory, the inconsistencies are expected at the country boarder of China and India. However, low populations and emissions are observed along the border of China, reducing the impact of cross-border grids on the accuracy of emissions. Also, deriving country totals from the gridded emissions is not appropriate for small countries due to the impact from cross-border grids, especially for those grids with large point source emissions (Janssens-Maenhout et al., 2015).

The current MIX inventory also has several limitations. Firstly, it provides emissions with aggregated sectoral information, which may be sufficient for the base case model but insufficient for targeted policy cases. Secondly, the MIX inventory is provided with moderate spatial resolution (i.e., 0.25° × 0.25°), which could support global and regional models but is still too coarse for urban models. Finally, yet importantly, gridded emissions are only available for 2008 and 2010 to support base years modeling activities in MICS-Asia and HTAP. For other years, modelers could use available global and regional inventories with more complete year coverage (e.g., EDGAR v4.2, REAS2) or extrapolate the gridded MIX inventory to the neighboring years. Developing a complete time series of gridded emission dataset with the best available local inventories is a challenging task because it requires extensive international collaboration to coordinate various resources. Continuous efforts under international collaboration frameworks (e.g., MICS-Asia, HTAP) could help to deliver improved and updated emission inventories over Asia continuously.

6 Concluding remarks

In this work, we developed a new anthropogenic emission inventory for Asia for the years of 2008 and 2010 by constructing a mosaic of several regional and national emission inventories. MEIC, PKU-NH$_3$, ANL-India, and CAPSS inventories are used to represent the best available emission data for China, India, and Korea, supplemented with REAS2 to fill gaps. By harmonizing these inventories, monthly emission grids maps for 10 species over Asia were generated for five sectors (power, industry, residential, transportation, and agriculture) at a uniform spatial resolution of 0.25° × 0.25°. Gridded speciated NMVOC emissions for SAPRC-99 and CB05 mechanisms were also developed at the same temporal and spatial resolution. This new Asian emission inventory, named MIX, provides model-ready anthropogenic emissions for the MICS-Asia Phase III assessment. The MIX inventory has been also incorporated into the HTAP v2 gridded emission inventory (Janssens-Maenhout et al., 2015) to support the TF HTAP assessment. Gridded emissions are available from the following website: http://www.meicmodel.org/dataset-mix.

The MIX inventory provides a consistent emission input for Asian regions for global and regional modeling activities. We expect that the MIX inventory can provide a good foundation for air quality modeling and can help to improve the model performance. However, the MIX inventory still has some limitations. It is very difficult to conduct quantitative uncertainty analysis for a mosaic inventory, which limits understanding of the reliability of the MIX inventory. Validation of the MIX inventory could be provided by comparing model predictions with in situ and satellite observations. The intercomparison between MIX and other inventories indicated that significantly different methodology and input data

were used in different emission inventories. Harmonizing the efforts among different regions and research groups through international collaborations could help to resolve this issue in the future.

7   Data availability

The monthly gridded emissions developed by this work can be accessed from http://www.meicmodel.org/dataset-mix at a spatial resolution of $0.25° × 0.25°$.

The Supplement related to this article is available online at doi:10.5194/acp-17-935-2017-supplement.

References

Adhikary, B., Carmichael, G. R., Kulkarni, S., Wei, C., Tang, Y., D'Allura, A., Mena-Carrasco, M., Streets, D. G., Zhang, Q., Pierce, R. B., Al-Saadi, J. A., Emmons, L. K., Pfister, G. G., Avery, M. A., Barrick, J. D., Blake, D. R., Brune, W. H., Cohen, R. C., Dibb, J. E., Fried, A., Heikes, B. G., Huey, L. G., O'Sullivan, D. W., Sachse, G. W., Shetter, R. E., Singh, H. B., Campos, T. L., Cantrell, C. A., Flocke, F. M., Dunlea, E. J., Jimenez, J. L., Weinheimer, A. J., Crounse, J. D., Wennberg, P. O., Schauer, J. J., Stone, E. A., Jaffe, D. A., and Reidmiller, D. R.: A regional scale modeling analysis of aerosol and trace gas distributions over the eastern Pacific during the INTEX-B field campaign, Atmos. Chem. Phys., 10, 2091–2115, doi:10.5194/acp-10-2091-2010, 2010.

Berezin, E. V., Konovalov, I. B., Ciais, P., Richter, A., Tao, S., Janssens-Maenhout, G., Beekmann, M., and Schulze, E.-D.: Multiannual changes of CO_2 emissions in China: indirect estimates derived from satellite measurements of tropospheric NO_2 columns, Atmos. Chem. Phys., 13, 9415–9438, doi:10.5194/acp-13-9415-2013, 2013.

Bond, T. C., Streets, D. G., Yarber, K. F., Nelson, S. M., Woo, J. H., and Klimont, Z.: A technology-based global inventory of black and organic carbon emissions from combustion, J. Geophys. Res., 109, D14203, doi:10.1029/2003jd003697, 2004.

Carmichael, G. R., Calori, G., Hayami, H., Uno, I., Cho, S. Y., Engardt, M., Kim, S. B., Ichikawa, Y., Ikeda, Y., Woo, J. H., Ueda, H., and Amann, M.: The MICS-Asia study: model intercomparison of long-range transport and sulfur deposition in East Asia, Atmos. Environ., 36, 175–199, 2002.

Carmichael, G. R., Tang, Y., Kurata, G., Uno, I., Streets, D., Woo, J. H., Huang, H., Yienger, J., Lefer, B., Shetter, R., Blake, D., Atlas, E., Fried, A., Apel, E., Eisele, F., Cantrell, C., Avery, M., Barrick, J., Sachse, G., Brune, W., Sandholm, S., Kondo, Y., Singh, H., Talbot, R., Bandy, A., Thorton, D., Clarke, A., and Heikes, B.: Regional-scale chemical transport modeling in support of the analysis of observations obtained during the TRACE-P experiment, J. Geophys. Res., 108, 8823, doi:10.1029/2002JD003117, 2003.

Carmichael, G. R., Sakurai, T., Streets, D., Hozumi, Y., Ueda, H., Park, S. U., Fung, C., Han, Z., Kajino, M., Engardt, M., Bennet, C., Hayami, H., Sartelet, K., Holloway, T., Wang, Z., Kannari, A., Fu, J., Matsuda, K., Thongboonchoo, N., and Amann, M.: MICS-Asia II: The model intercomparison study for Asia Phase II methodology and overview of findings, Atmos. Environ., 42, 3468–3490, 2008.

Carter, W. P. L.: Documentation of the SAPRC-99 chemical mechanism for VOC reactivity assessment, report to the California Air Resources Board, available at: http://www.engr.ucr.edu/~carter/reactdat.htm (last access: October 2013), 2000.

Carter, W. P. L.: Development of an improved chemical speciation database for processing emissions of volatile organic compounds for air quality models, report available at: http://www.engr.ucr.edu/~carter/emitdb/ (last access: November 2013), 2013.

EC-JRC/PBL (European Commission, Joint Research Center/Netherlands Environmental As- sessment Agency), Emission Database for Global Atmospheric Research version 4.2, available at: http://edgar.jrc.ec.europa.eu (last access: June 2015), 2011.

Fortems-Cheiney, A., Chevallier, F., Pison, I., Bousquet, P., Szopa, S., Deeter, M. N., and Clerbaux, C.: Ten years of CO emissions as seen from Measurements of Pollution in the Troposphere (MOPITT), J. Geophys. Res., 116, D05304, doi:10.1029/2010JD014416, 2011.

Garg, A., Shukla, P. R., Bhattacharya, S., and Dadhwal, V. K.: Subregion (district) and sector SO_2 and NO_x emissions for India: assessment of inventories and mitigation flexibility, Atmos. Environ., 35, 703–713, 2001.

Garg, A., Shukla, P. R., and Kapshe, M.: The sectoral trends of multigas emissions inventory of India, Atmos. Environ., 40, 4608–4620, 2006.

Granier, C., Bessagnet, B., Bond, T., D'Angiola, A., Denier van der Gon, H., Frost, G., Heil, A., Kaiser, J., Kinne, S., Klimont, Z., Kloster, S., Lamarque, J.-F., Liousse, C., Masui, T., Meleux, F., Mieville, A., Ohara, T., Raut, J.-C., Riahi, K., Schultz, M., Smith, S., Thompson, A., van Aardenne, J., van der Werf, G., and van Vuuren, D.: Evolution of anthropogenic and biomass burning emissions of air pollutants at global and regional scales during the 1980–2010 period, Climatic Change, 109, 163–190, doi:10.1007/s10584-011-0154-1, 2011.

Gu, D., Wang, Y. H., Smeltzer, C., and Liu, Z.: Reduction in NOx emission trends over China: regional and seasonal variations, Environ. Sci. Technol., 47, 12912–12919, 2013.

Guan, D., Liu, Z., Geng, Y., Lindner, S., and Hubacek, K.: The gigatonne gap in China's carbon dioxide inventories, Nature Clim. Change, 2, 672–675, 2012.

Habib, G., Venkataraman, C., Shrivastava, M., Banerjee, R., Stehr, J. W., and Dickerson, R. R.: New methodology for estimating biofuel consumption for cooking: Atmospheric emissions of black carbon and sulfur dioxide from India, Global Biogeochem. Cy., 18, GB3007, doi:10.1029/2003GB002157, 2004.

Han, Z., Sakurai, T., Ueda, H., Carmichael, G. R., Streets, D., Hayami, H., Wang, Z., Holloway, T., Engardt, M., Hozumi, Y., Park, S. U., Kajino, M., Sartelet, K., Fung, C., Bennet, C., Thongboonchoo, N., Tang, Y., Chang, A., Matsuda, K., and Amann, M.: MICS-Asia II: Model intercomparison and evaluation of ozone and relevant species, Atmos. Environ., 42, 3491–3509, doi:10.1016/j.atmosenv.2007.07.031, 2008.

Hayami, H., Sakurai, T., Han, Z., Ueda, H., Carmichael, G. R., Streets, D., Holloway, T., Wang, Z., Thongboonchoo, N., Engardt, M., Bennet, C., Fung, C., Chang, A., Park, S. U., Kajino, M., Sartelet, K., Matsuda, K., and Amann, M.: MICS-Asia II: Model intercomparison and evaluation of particulate sulfate, nitrate and ammonium, Atmos. Environ., 42, 3510–3527, doi:10.1016/j.atmosenv.2007.08.057, 2008.

He, Y., Uno, I., Wang, Z., Ohara, T., Sugimoto, N., Shimizu, A., Richter, A., and Burrows, J. P.: Variations of the increasing trend of tropospheric NO_2 over central east China during the past decade, Atmos. Environ., 41, 4865–4876, 2007.

Holloway, T., Sakurai, T., Han, Z., Ehlers, S., Spak, S. N., Horowitz, L. W., Carmichael, G. R., Streets, D. G., Hozumi, Y., Ueda, H., Park, S. U., Fung, C., Kajino, M., Thongboonchoo, N., Engardt, M., Bennet, C., Hayami, H., Sartelet, K., Wang, Z., Matsuda, K., and Amann, M.: MICS-Asia II: Impact of global emissions on regional air quality in Asia, Atmos. Environ., 42, 3543–3561, doi:10.1016/j.atmosenv.2007.10.022, 2008.

Hong, C., Zhang, Q., He, K., Guan, D., Li, M., Liu, F., and Zheng, B.: Variations of China's emission estimates response to uncertainties in energy statistics, Atmos. Chem. Phys. Discuss., doi:10.5194/acp-2016-459, in review, 2016.

Hsu, Y. and Divita, F.: SPECIATE 4.2, speciation database development documentation, final report, EPA/600-R-09/-38, 2009.

Huang, X., Song, Y., Li, M., Li, J., Huo, Q., Cai, X., Zhu, T., Hu, M., and Zhang, H.: A high-resolution ammonia emission inventory in China, Global Biogeochem. Cy., 26, GB1030, doi:10.1029/2011GB004161, 2012.

IEA (International Energy Agency): Energy balances of OECD countries and energy balances of non-OECD countries, CD-ROM, IEA, Paris, 2013.

Itahashi, S., Uno, I., Irie, H., Kurokawa, J.-I., and Ohara, T.: Regional modeling of tropospheric NO_2 vertical column density over East Asia during the period 2000–2010: comparison with multisatellite observations, Atmos. Chem. Phys., 14, 3623–3635, doi:10.5194/acp-14-3623-2014, 2014.

Janssens-Maenhout, G., Crippa, M., Guizzardi, D., Dentener, F., Muntean, M., Pouliot, G., Keating, T., Zhang, Q., Kurokawa, J., Wankmüller, R., Denier van der Gon, H., Kuenen, J. J. P., Klimont, Z., Frost, G., Darras, S., Koffi, B., and Li, M.: HTAP_v2.2: a mosaic of regional and global emission grid maps for 2008 and 2010 to study hemispheric transport of air pollution, Atmos. Chem. Phys., 15, 11411–11432, doi:10.5194/acp-15-11411-2015, 2015.

JPEC (Japan Petroleum Energy Center): Emission inventory of road transport in Japan, JPEC Technical Report, JPEC-2011AQ-02-06, 136 pp., 2012a (in Japanese).

JPEC: Emission inventory of sources other than road transport in Japan, JPEC Technical Report, JPEC-2011AQ-02-07, 288 pp., 2012b (in Japanese).

JPEC: Speciation profiles of VOC, PM, and NOx emissions for atmospheric simulations of PM2.5, JPEC Technical Report, JPEC-2011AQ-02-08, 69 pp., 2012c (in Japanese).

Kannari, A., Tonooka, Y., Baba, T., and Murano, K.: Development of multiple-species $1\,km \times 1\,km$ resolution hourly basis emissions inventory for Japan, Atmos. Environ., 41, 3428–3439, 2007.

Keller, C. A., Long, M. S., Yantosca, R. M., Da Silva, A. M., Pawson, S., and Jacob, D. J.: HEMCO v1.0: a versatile, ESMF-compliant component for calculating emissions in atmospheric models, Geosci. Model Dev., 7, 1409–1417, doi:10.5194/gmd-7-1409-2014, 2014.

Klimont, Z.: Current and future emissions of ammonia in China, in: Proceedings of 10th International Emission Inventory Conference – "One Atmosphere, One Inventory, Many Challenges", Denver, US, 1–3 May, Sect. 1, 5, 2001.

Klimont, Z., Streets, D. G., Gupta, S., Cofala, J., Fu, L. X., and Ichikawa, Y.: Anthropogenic emissions of non-methane volatile organic compounds in China, Atmos. Environ., 36, 1309–1322, doi:10.1016/s1352-2310(01)00529-5, 2002.

Krotkov, N. A., McLinden, C. A., Li, C., Lamsal, L. N., Celarier, E. A., Marchenko, S. V., Swartz, W. H., Bucsela, E. J., Joiner, J., Duncan, B. N., Boersma, K. F., Veefkind, J. P., Levelt, P. F., Fioletov, V. E., Dickerson, R. R., He, H., Lu, Z., and Streets, D. G.: Aura OMI observations of regional SO_2 and NO_2 pollution changes from 2005 to 2015, Atmos. Chem. Phys., 16, 4605–4629, doi:10.5194/acp-16-4605-2016, 2016.

Kurokawa, J.-I., Yumimoto, K., Uno, I., and Ohara, T.: Adjoint inverse modeling of NOx emissions over eastern China using satellite observations of NO2 vertical column densities, Atmos. Environ., 43, 1878–1887, 2009.

Kurokawa, J., Ohara, T., Morikawa, T., Hanayama, S., Janssens-Maenhout, G., Fukui, T., Kawashima, K., and Akimoto, H.: Emissions of air pollutants and greenhouse gases over Asian regions during 2000–2008: Regional Emission inventory in ASia (REAS) version 2, Atmos. Chem. Phys., 13, 11019–11058, doi:10.5194/acp-13-11019-2013, 2013.

Lee, D. G., Lee, Y.-M., Jang, K.-W., Yoo, C., Kang, K.-H., Lee, J.-H., Jung, S.-W., Park, J.-M., Lee, S.-B., Han, J.-S., Hong, J.-H., and Lee, S.-J.: Korean national emissions inventory system and 2007 air pollutant emissions, Asian J. Atmos. Environ., 5, 278–291, 2011.

Lei, Y., Zhang, Q., He, K. B., and Streets, D. G.: Primary anthropogenic aerosol emission trends for China, 1990–2005, Atmos. Chem. Phys., 11, 931–954, doi:10.5194/acp-11-931-2011, 2011.

Li, C., Marufu, L. T., Dickerson, R. R., Li, Z., Wen, T., Wang, Y., Wang, P., Chen, H., and Stehr, J. W.: In situ measurements of trace gases and aerosol optical properties at a rural site in northern China during East Asian Study of Tropospheric Aerosols: An International Regional Experiment 2005, J. Geophys. Res., 112, D22S04, doi:10.1029/2006JD007592, 2007.

Li, M., Zhang, Q., Streets, D. G., He, K. B., Cheng, Y. F., Emmons, L. K., Huo, H., Kang, S. C., Lu, Z., Shao, M., Su, H., Yu, X.,

and Zhang, Y.: Mapping Asian anthropogenic emissions of non-methane volatile organic compounds to multiple chemical mechanisms, Atmos. Chem. Phys., 14, 5617–5638, doi:10.5194/acp-14-5617-2014, 2014.

Lin, J. T., Nielsen, C. P., Zhao, Y., Lei, Y., Liu, Y., and McElroy, M. B.: Recent changes in particulate air pollution over China observation from space and the ground: effectiveness of emission control, Environ. Sci. Technol., 44, 7771–7776, 2010.

Liu, F., Zhang, Q., Tong, D., Zheng, B., Li, M., Huo, H., and He, K. B.: High-resolution inventory of technologies, activities, and emissions of coal-fired power plants in China from 1990 to 2010, Atmos. Chem. Phys., 15, 13299–13317, doi:10.5194/acp-15-13299-2015, 2015.

Lu, Z. and Streets, D. G.: Increase in NOx Emissions from Indian Thermal Power Plants during 1996–2010: Unit-Based Inventories and Multisatellite Observations, Environ. Sci. Technol., 46, 7463–7470, doi:10.1021/es300831w, 2012.

Lu, Z., Zhang, Q., and Streets, D. G.: Sulfur dioxide and primary carbonaceous aerosol emissions in China and India, 1996–2010, Atmos. Chem. Phys., 11, 9839–9864, doi:10.5194/acp-11-9839-2011, 2011.

Mijling, B., van der A, R. J., and Zhang, Q.: Regional nitrogen oxides emission trends in East Asia observed from space, Atmos. Chem. Phys., 13, 12003–12012, doi:10.5194/acp-13-12003-2013, 2013.

Miyazaki, K., Eskes, H., Sudo, K., Boersma, K. F., Bowman, K., and Kanaya, Y.: Decadal changes in global surface NO_x emissions from multi-constituent satellite data assimilation, Atmos. Chem. Phys. Discuss., doi:10.5194/acp-2016-529, in review, 2016.

Ohara, T., Akimoto, H., Kurokawa, J., Horii, N., Yamaji, K., Yan, X., and Hayasaka, T.: An Asian emission inventory of anthropogenic emission sources for the period 1980–2020, Atmos. Chem. Phys., 7, 4419–4444, doi:10.5194/acp-7-4419-2007, 2007.

OPRF (Ocean Policy Research Foundation (Ship and Ocean Foundation)): Report for comprehensive study for environmental impact lead by the establishment of emission control area in Japan, ISBN-13: 978-4-88404-282-0, 524 pp., 2012 (in Japanese).

Paulot, F., Jacob, D. J., Pinder, R. W., Bash, J. O., Travis, K., and Henze, D. K.: Ammonia emissions in the United States, European Union, and China derived by high-resolution inversion of ammonium wet deposition data: Interpretation with a new agricultural emissions inventory (MASAGE_NH3), J. Geophys. Res., 119, 4343–4364, doi:10.1002/2013JD021130, 2014.

Pétron, G., Granier, C., Khattatov, B., Yudin, V., Lamarque, J.-F., Emmons, L., Gille, J., and Edwards, D. P.: Monthly CO surface sources inventory based on the 2000–2001 MOPITT satellite data, Geophys. Res. Lett., 31, L21107, doi:10.1029/2004GL020560, 2004.

Platts: The UDI Word Electric Power Plants Database, CD-ROM data, Platts, A division of the McGraw-Hill Companies, New York, 2009.

Reddy, M. S. and Venkataraman, C.: Inventory of aerosol and sulphur dioxide emissions from India: I – Fossil fuel combustion, Atmos. Environ., 36, 677–697, 2002a.

Reddy, M. S. and Venkataraman, C.: Inventory of aerosol and sulphur dioxide emissions from India. Part II – biomass combustion, Atmos. Environ., 36, 699–712, 2002b.

Simon, H., Beck, L., Bhave, P. V., Divita, F., Hsu, Y., Luecken, D., Mobley, J. D., Pouliot, G. A., Reff, A., Sarwar, G., and Strum, M.: The development and uses of EPA's SPECIATE database, Atmos. Pollut. Res., 1, 196–206, 2010.

Streets, D. G., Bond, T. C., Carmichael, G. R., Fernandes, S. D., Fu, Q., He, D., Klimont, Z., Nelson, S. M., Tsai, N. Y., Wang, M. Q., Woo, J. H., and Yarber, K. F.: An inventory of gaseous and primary aerosol emissions in Asia in the year 2000, J. Geophys. Res., 108, 8809, doi:10.1029/2002JD003093, 2003.

Streets, D. G., Zhang, Q., Wang, L., He, K., Hao, J., Wu, Y., Tang, Y., and Carmichael, G. R.: Revisiting China's CO emissions after the Transport and Chemical Evolution over the Pacific (TRACE-P) mission: Synthesis of inventories, atmospheric modeling, and observations, J. Geophys. Res.-Atmos., 111, D14306, doi:10.1029/2006JD007118, 2006.

Streets, D. G., Canty, T., Carmichael, G. R., de Foy, B., Dickerson, R. R., Duncan, B. N., Edwards, D. P., Haynes, J. A., Henze, D. K., Houyoux, M. R., Jacob, D. J., Krotkov, N. A., Lamsal, L. N., Liu, Y., Lu, Z., Martin, R. V., Pfister, G. G., Pinder, R. W., Salawitch, R. J., and Wecht, K. J.: Emissions estimation from satellite retrievals: A review of current capability, Atmos. Environ., 77, 1011–1042, doi:10.1016/j.atmosenv.2013.05.051, 2013.

United Nations: Monthly Bulletin of Statistics (MBS), United Nations Publications, New York, 341 pp., 2011.

van Donkelaar, A., Martin, R. V., Leaitch, W. R., Macdonald, A. M., Walker, T. W., Streets, D. G., Zhang, Q., Dunlea, E. J., Jimenez, J. L., Dibb, J. E., Huey, L. G., Weber, R., and Andreae, M. O.: Analysis of aircraft and satellite measurements from the Intercontinental Chemical Transport Experiment (INTEX-B) to quantify long-range transport of East Asian sulfur to Canada, Atmos. Chem. Phys., 8, 2999–3014, doi:10.5194/acp-8-2999-2008, 2008.

Venkataraman, C., Habib, G., Eiguren-Fernandez, A., Miguel, A. H., and Friedlander, S. K.: Residential biofuels in South Asia: carbonaceous aerosol emissions and climate impacts, Science, 307, 1454–1456, 2005.

Wang, S. W., Zhang, Q., Streets, D. G., He, K. B., Martin, R. V., Lamsal, L. N., Chen, D., Lei, Y., and Lu, Z.: Growth in NOx emissions from power plants in China: bottom-up estimates and satellite observations, Atmos. Chem. Phys., 12, 4429–4447, doi:10.5194/acp-12-4429-2012, 2012.

Wang, Y., Munger, J. W., Xu, S., McElroy, M. B., Hao, J., Nielsen, C. P., and Ma, H.: CO_2 and its correlation with CO at a rural site near Beijing: implications for combustion efficiency in China, Atmos. Chem. Phys., 10, 8881–8897, doi:10.5194/acp-10-8881-2010, 2010.

Wang, Y., Zhang, Q. Q., He, K., Zhang, Q., and Chai, L.: Sulfate-nitrate-ammonium aerosols over China: response to 2000–2015 emission changes of sulfur dioxide, nitrogen oxides, and ammonia, Atmos. Chem. Phys., 13, 2635–2652, doi:10.5194/acp-13-2635-2013, 2013.

Wang, Z., Xie, F., Sakurai, T., Ueda, H., Han, Z., Carmichael, G. R., Streets, D., Engardt, M., Holloway, T., Hayami, H., Kajino, M., Thongboonchoo, N., Bennet, C., Park, S. U., Fung, C., Chang, A., Sartelet, K., and Amann, M.: MICS-Asia II: Model intercomparison and evaluation of acid deposition, Atmos. Environ., 42, 3528–3542, doi:10.1016/j.atmosenv.2007.12.071, 2008.

Wheeler, D. and Ummel, K.: Calculating CARMA: Global estimation of CO_2 emissions from the power sector, Center for Global Development, Working Paper 145, 2008.

Woo, J.-H., Choi, K.-C., Kim, H. K., Baek, B. H., Jang, M., Eum, J.-H., Song, C. H., Ma, Y., Sunwoo, Y., Chang, L.-S., and Yoo, S. H.: Development of an anthropogenic emissions processing system for Asia using SMOKE, Atmos. Environ., 58, 5–13, 2012.

Worden, H. M., Deeter, M. N., Frankenberg, C., George, M., Nichitiu, F., Worden, J., Aben, I., Bowman, K. W., Clerbaux, C., Coheur, P. F., de Laat, A. T. J., Detweiler, R., Drummond, J. R., Edwards, D. P., Gille, J. C., Hurtmans, D., Luo, M., Martínez-Alonso, S., Massie, S., Pfister, G., and Warner, J. X.: Decadal record of satellite carbon monoxide observations, Atmos. Chem. Phys., 13, 837–850, doi:10.5194/acp-13-837-2013, 2013.

World Steel Association: Steel Statistical Yearbook 2011, worldsteel Committee on Economic Studies, Brussels, 120 pp., 2011.

Xing, J., Pleim, J., Mathur, R., Pouliot, G., Hogrefe, C., Gan, C.-M., and Wei, C.: Historical gaseous and primary aerosol emissions in the United States from 1990 to 2010, Atmos. Chem. Phys., 13, 7531–7549, doi:10.5194/acp-13-7531-2013, 2013.

Yarwood, G., Rao, S., Yocke, M., and Whitten, G.: Updates to the Carbon Bond Chemical Mechanism: CB05, Final Report to the US EPA, RT-0400675, available at: http://www.camx.com (last access: October 2013), 2005.

Yin, Y., Chevallier, F., Ciais, P., Broquet, G., Fortems-Cheiney, A., Pison, I., and Saunois, M.: Decadal trends in global CO emissions as seen by MOPITT, Atmos. Chem. Phys., 15, 13433–13451, doi:10.5194/acp-15-13433-2015, 2015.

Yumimoto, K., Uno, I., and Itahashi, S.: Long-term inverse modeling of Chinese CO emission from satellite observations, Environ. Pollut., 195, 308–318, 2014.

Zhang, Q., Streets, D. G., He, K., and Klimont, Z.: Major components of China's anthropogenic primary particulate emissions, Environ. Res. Lett., 2, 045027, doi:10.1088/1748-9326/2/4/045027, 2007a.

Zhang, Q., Streets, D. G., He, K. B., Wang, Y. X., Richter, A., Burrows, J. P., Uno, I., Jang, C. J., Chen, D., Yao, Z., and Lei, Y.: NO_x emission trends for China, 1995–2004: The view from the ground and the view from space, J. Geophys. Res., 112, D22306, doi:10.1029/2007JD008684, 2007b.

Zhang, Q., Streets, D. G., Carmichael, G. R., He, K. B., Huo, H., Kannari, A., Klimont, Z., Park, I. S., Reddy, S., Fu, J. S., Chen, D., Duan, L., Lei, Y., Wang, L. T., and Yao, Z. L.: Asian emissions in 2006 for the NASA INTEX-B mission, Atmos. Chem. Phys., 9, 5131–5153, doi:10.5194/acp-9-5131-2009, 2009.

Zhang, Q., He, K., and Huo, H.: Policy: Cleaning China's air, Nature, 484, 161–162, 2012.

Zhao, Y., Nielsen, C. P., Lei, Y., McElroy, M. B., and Hao, J.: Quantifying the uncertainties of a bottom-up emission inventory of anthropogenic atmospheric pollutants in China, Atmos. Chem. Phys., 11, 2295–2308, doi:10.5194/acp-11-2295-2011, 2011.

Zhao, Y., Zhang, J., and Nielsen, C. P.: The effects of recent control policies on trends in emissions of anthropogenic atmospheric pollutants and CO_2 in China, Atmos. Chem. Phys., 13, 487–508, doi:10.5194/acp-13-487-2013, 2013.

Zheng, B., Huo, H., Zhang, Q., Yao, Z. L., Wang, X. T., Yang, X. F., Liu, H., and He, K. B.: High-resolution mapping of vehicle emissions in China in 2008, Atmos. Chem. Phys., 14, 9787–9805, doi:10.5194/acp-14-9787-2014, 2014.